High-Resolution Seismic-Reflection Study of the Anthropogenic Leesburg Sinkhole in Stafford County, Kansas

Rick Miller

Kansas Geological Survey
1930 Constant Avenue
Lawrence, Kansas 66047

Report to
Doug Louis, Kansas Corporation Commission, Conservation Division, Wichita, Kansas 67202

Open-file Report No. 2009-1

July 2008

High-Resolution Seismic-Reflection Study of the Anthropogenic Leesburg Sinkhole in Stafford County, Kansas

by
Richard D. Miller
Kansas Geological Survey, 1930 Constant Avenue, Lawrence, Kansas

for
Doug Louis
Kansas Corporation Commission, Conservation Division
Wichita, Kansas

SUMMARY

High-resolution seismic reflections were used to map rock layers in the first 2000 ft below ground surface around and below the Leesburg sinkhole in Stafford County, Kansas. Two approximately mile-long seismic reflection profiles, nearly orthogonal, intersected the sinkhole located approximately 5 miles west and 4.5 miles south of Stafford, Kansas. The seismic data allowed the mapping of key rock layers in the upper 2000 ft, providing a glimpse at this very asymmetric and developing subsidence feature. Based on geologic and geophysical interpretations of these data, preferential growth directions and vertical extent can he estimated. It was also possible from these data to identify a subsidence feature separate and distinct from the current sinkhole yet to form a surface depression. The high signal quality and resolution of these seismic-reflection data permitted detection, delineation, and evaluation of all the major rock units associated with the sinkhole.

At this location unsaturated brine waters have gained access to the approximately 1000-ft-deep, 400-ft-thick Permian-aged Hutchinson Salt Member of the Wellington Formation. Oil-field casing provided the conduit for disposal fluids and ground water to gain access to the salt interval. Voids formed by the leaching of salt hy these fluids grew to the point they exceeded the strength of the roof rock, resulting in overburden failure and the migration of the void to the ground surface. Seismically imaged Permian-aged rocks and Quaternary sediments that overlay the salt in this area provide the clues to the collapse chronology and allow some level of confidence in predicting future growth.

Mechanisms and gross chronology of structural failures interpreted on seismic sections indicate initial subsidence and associated rock failure occurred as accumulated stress on roof rocks spanning salt voids exceeded the strength in roof rock. A chimney-like feature, narrowing upward from its widest point at the top of salt, formed as a result of this roof-rock failure. From these seismic sections, acquired in 2004, it is clear that the bed offset is controlled by several reverse faults, subparallel and expanding outwards from the center pair, that define the initial narrow chimney. Clearly at the time the data were collected, dissolution along the northern edge was minimal to nonexistent. The eastern and southern portions of the feature appear to most likely be experiencing active dissolution and therefore have the greatest future subsidence potential. The rate of destabilization and failure as well as the load-bearing potential of the rock layers above zones of dissolution strongly influence the subsidence geometries. Most unusual about the seismic images of this anthropogenic sinkhole is the lack of symmetry.

With active fluid movement through well casings at this site, subsidence will continue, only changing as access to the salt interval is altered from collapse breccia resulting from the upward movement of dissolution voids. It is unlikely surface subsidence will progress at rates greater than those documented over the last 10 years. Sufficient bridging and undercompacted rock layers still exist beneath this sinkhole to sustain the current subsidence rate for several years to come without any future leaching of the salt.

Introduction

Sinkholes are common hazards to property and human safety the world over (Beck et al., 1999). Their formation is generally associated with subsurface subsidence that occurs when overburden loads exceed the strength of the roof rock bridging voids or rubble zones formed as a result of dissolution or mining. Understanding sinkhole processes and what controls their formation rate is key to reducing their impact on human activities, and in the case of anthropogenic causes, potentially avoiding their formation altogether. Sinkholes can form naturally or anthropogenically from the dissolution of limestone (karst), gypsum, or rock salt, or from mine/tunnel collapse. With the worldwide abundance of limestone, karst-related sinkholes are by far the most commonly encountered and studied. Both simple and complex sinkholes have formed catastrophically and/or gradually, as the result of dissolution of limestone or rock salt, and by natural and human-induced dissolution processes in many parts of Kansas (Merriam and Mann, 1957).

In central Kansas most sinkholes are the result of leached-out volumes of the Permian Hutchinson Salt Member of the Wellington Formation (Watney et al., 1988). Sinkholes forming above salt layers have been studied throughout Kansas (Frye, 1950; Walters, 1978) and the United States (Ege, 1984). Studies of subsidence related to mining of the salt around Hutchinson, Kansas (Walters, 1980), disposal of oil-field brine near Russell, Kansas (Walters, 1991), and natural dissolution through fault/fracture-induced permeability (Frye and Schoff, 1942) have drawn conclusions about the mechanism responsible for subsidence geometries and rates based on surface and/or borehole observations. Using only surface observations and borehole data, a great number of assumptions and a good deal of geologic/mechanical sense must be drawn on to define and explain these features and their impact. High-resolution seismic-reflection profiling has proven an effective tool in 3-D mapping of the subsurface expression and predicting future surface deformation associated with dissolution of the Hutchinson Salt Member in Kansas (Steeples et al., 1986; Miller et al., 1993; Anderson et al., 1995a; Miller et al., 1995; Miller et al., 1997).

Salt-dissolution sinkholes are found in all areas of Kansas where the Hutchinson Salt Member is present in the subsurface. Sinkholes have been definitely correlated to failed containment of disposal wells injecting oil-field-brine wastewater using stem-pressure tests and/or seismic-reflection investigations at a variety of sites throughout central Kansas (Steeples et al., 1986; Knapp et al., 1989; Miller et al., 1995; Miller et al., 1997). Sinkholes that have formed by natural dissolution and subsidence processes are most commonly documented at the depositional edges on the west and north and erosional boundary on the east of the Hutchinson Salt Member (Frye and Schoff, 1942; Frye, 1950; Merriam and Mann, 1957; Anderson et al., 1995a). The vast majority of published works studying the source of localized leaching of salt in Kansas directly contradict suggestions that recent land subsidence in Kansas is mostly natural in origin (Anderson et al., 1995a).

Natural dissolution of the Hutchinson Salt Member is not uncommon in Kansas and has been occurring for millions of years (Ege, 1984). Faults extending up to Pleistocene sediments containing fresh water under hydrostatic pressure are postulated as the conduits instigating salt dissolution and subsidence along the western boundary of the salt in Kansas (Frye and Schoff, 1942). Paleosinkholes resulting from dissolution of the salt before Pleistocene deposition have been discovered previously with high-resolution seismic surveys (Anderson et al., 1998).

Subsidence can occur at rates ranging from gradual to catastrophic. Subsidence rates are to some extent related to the dimensions (including the ratio of vertical to horizontal) of the dissolution void, depth to the roof of the void, and the strength of rocks immediately above the salt layer. As salt is leached, the resulting pore space provides the differential pressure necessary to support creep (Carter and Hansen, 1983). If this pore space gets large enough to exceed the strength of the roof rock, the unsupported span will fail and subsidence occurs. Depending on the strength of the roof rock and therefore the size of the void, characteristics of the failure within and just above the salt will dictate how the void progresses upward until it eventually reaches the ground surface. In general, gradual surface subsidence is associated with an ever-growing howl-shaped depression with bed geometries and offsets constrained by normal fault geometries which have followed initial compressional failure of the void roof (Steeples et al., 1986; Anderson et al., 1995b). When rapid to catastrophic subsidence rates are observed, failure within the salt is brittle and compressional with the void volume migrating to the surface as an ever-narrowing cone with bed offsets and rock failure controlled by reverse-type fault planes (Davies, 1951; Walters 1980; Rokar and Staudtmeister, 1985).

Seismic-reflection data targeting beds altered by dissolution and subsidence in this area have ranged in quality and interpretability from poor (Miller et al., 1995) to outstanding (Miller et al., 1997). Interpretations when data quality is poor have unfortunately been relegated to indirect inference of structural processes and subsurface expression (mainly from interpretations of structural deformation in layers above the salt) due to low signal-to-noise ratios. However, data with excellent signal-to-noise ratios and resolution have allowed direct detection of structures and geometries that appear characteristic of complex sinkholes. Resolution potential and signal-to-noise ratio of seismic data from this study are superior to any previously published that have targeted the salt interval. These data provide conclusive images of important structural features and unique characteristics that control sinkhole development.

The Leeshurg sinkhole is offset to the west of Stafford County Road 503 and is 4½ miles south of U.S. 50 in Stafford County, Kansas (Figure 1). Lost containment in a disposal well initiated an effort to plug the disposal well. Failure to plug the well and the known movement of water vertically outside the casing leaves little doubt as to the origin of the fluids that leached the salt at this site. Two orthogonal seismic profiles clearly display a highly altered and nonsymmetric collapse structure significantly larger than the surface feature. The two seismic profiles possess evidence of more than one structure above salt.

Geologic Setting

Several major salt basins exist throughout North America (Ege, 1984). The Hutchinson Salt Member occurs in central Kansas, northwestern Oklahoma, and the northeastern portion of the Texas Panhandle, and is prone to and has an extensive history of dissolution and formation of sinkholes (Figure 1). In Kansas, the Hutchinson Salt Member possesses an average net thickness of 250 ft and reaches a maximum of over 400 ft in the southern part of the basin. Deposition

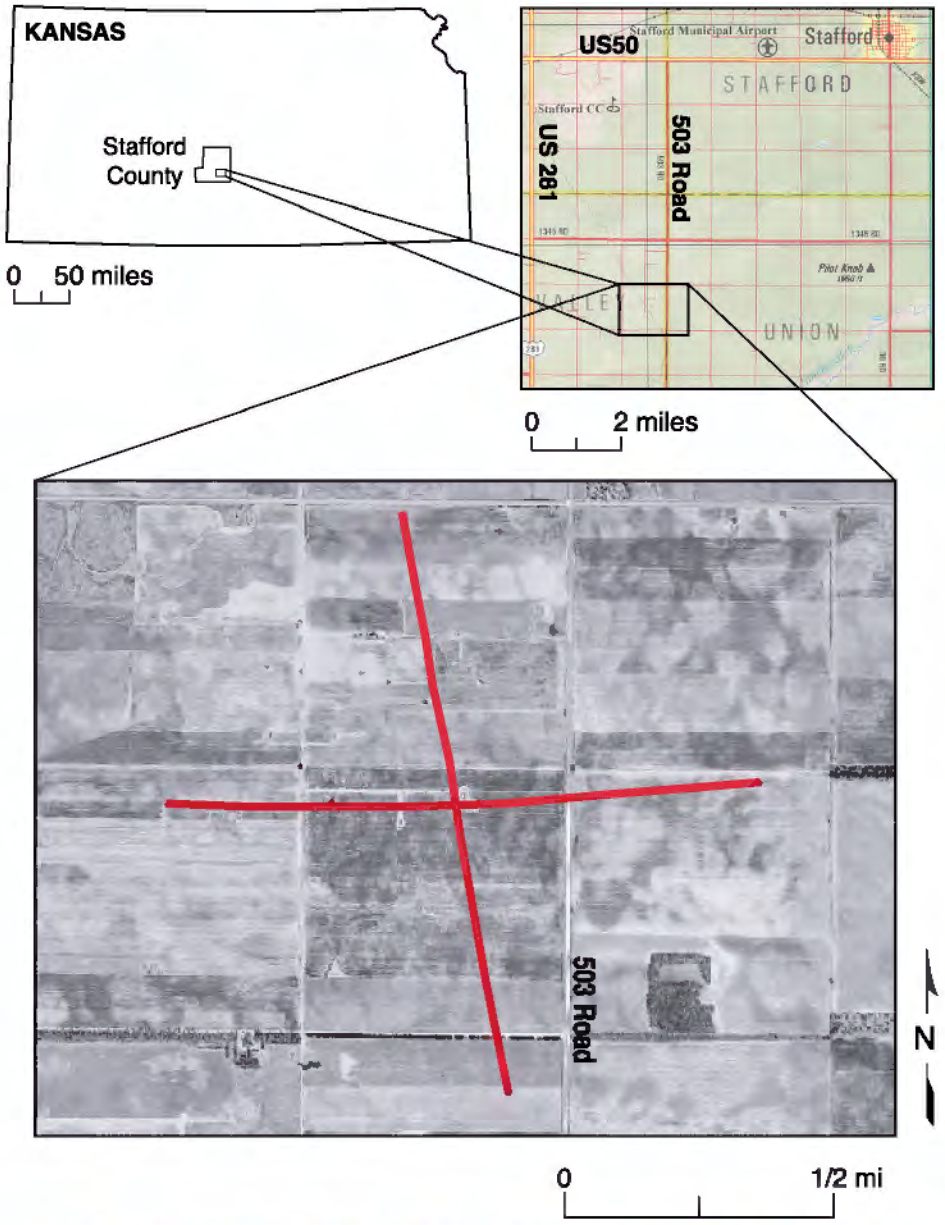

Figure 1. Maps showing location of Leesburg sinkhole and seismic lines.

occurring during fluctuating sea levels caused numerous halite beds, 1 to 10 ft thick, to be formed interbedded with shale, minor anhydrite, and dolomite/magnesite. Individual salt beds may be continuous for only a few miles despite the remarkable lateral continuity of the salt as a whole (Walters, 1978).

Rock salt under a depositional load is almost incompressible, highly ductile, and easily deformed by creep (Baar, 1977). Plastic deformation of the salt associated with creep is expected naturally to occur in these salts (Anderson et al., 1995b). Thin anhydrite beds within the halite succession have a strong acoustic response. Considering the extreme range of possible strain rates the salt can experience during creep deformation, these thin interbeds can possess quite dramatic, high-frequency folds within relatively short distances.

Red-bed evaporites overlaying the Hutchinson Salt Member are a primary target of any study in Kansas looking at salt-dissolution sinkhole development and associated risks to the environment and human activity. Failure and subsidence of these evaporite units are responsible for the eventual formation of sinkholes and provide a pathway for ground water to gain access to the salt. In proximity to the dissolution front, fractures, faults, and collapse structures compromise the confining properties of the Permian shale bedrock and put the major freshwater aquifer (Pliocene-Pleistocene Equus beds) in this part of southern Kansas at risk. Along the eastern houndary (dissolution front) the salt, which ranges from 0 to over 300 ft thick, is buried beneath about 400 ft of Permian red-bed evaporites.

The eastern margin of the salt was exposed during the late Tertiary where erosion and leaching began the 20-mile westward progression of the front to its present-day location (Bayne, 1956). The ability of the front to migrate while under as much as 300 ft of sediments was a direct consequence of ready access to an abundant supply of ground water (Watney et al., 1988). Subsidence of Permian, Cretaceous, and Tertiary rocks has progressed along the migration front as the salt has been leached away. While this subsidence was going on, Quaternary alluvium was being deposited in volumes consistent with the salt that was being removed. This process resulted in today's moderate to low surface relief that masks the extremely distorted (faulted and folded—nontectonic) rock layers within the upper Wellington and Ninnescah shales (Anderson et al., 1998).

Seismically all the Permian and younger reflectors are important to the accurate interpretation of the stacked sections. Model studies show significant time delays (static) and geometric distortions that are to be expected below recent subsidence (Anderson et al., 1995b). "Pull downs" in time result from the localized decreases in material velocities within a sinkhole. The velocity structure and small radius of curvature of the synforms, which are characteristic of salt dissolution and subsidence in this area, can produce diffractions and distort reflections on vertically incident reflection sections. Reflections from beneath the salt will have a subdued expression of the post-salt subsidence. Estimations of subsidence and therefore volume of rock salt removed based on time-section estimations alone (without compensation for velocity variability) may exceed actual by as much as 25 to 50 percent in this area. Considering this geologic setting, it is reasonable to compensate for compaction-related static causing this lateral decrease in velocity by "flattening" on the top of the Chase Group.

Seismic Acquisition

To ensure the entire subsurface "root" of the sinkhole was clearly imaged, the survey was designed with two seismic lines, each possessing at least 1 mile of full-fold subsurface coverage nearly centered on the sinkhole (Figure 2). With the sinkhole located within an open agricultural field, two orthogonal seismic lines could be acquired with minimal surface obstructions. These data were acquired using a rolling fixed-spread design that eliminated the need for a roll-along switch and extended the range of far offsets availahle during processing. This survey design provided the wide range of source offsets necessary for detailed velocity analysis, allowed close receiver spacing for improved confidence in event identification, and maximized the range of imageable depths.

Even if the sinkhole visible at the ground surface is the result of a single gradual failure event, it is but a subdued, miniature expression of the subterranean disturbed rock layers at and below bedrock. Based on seismic-reflection surveys, all sinkholes that have formed from the

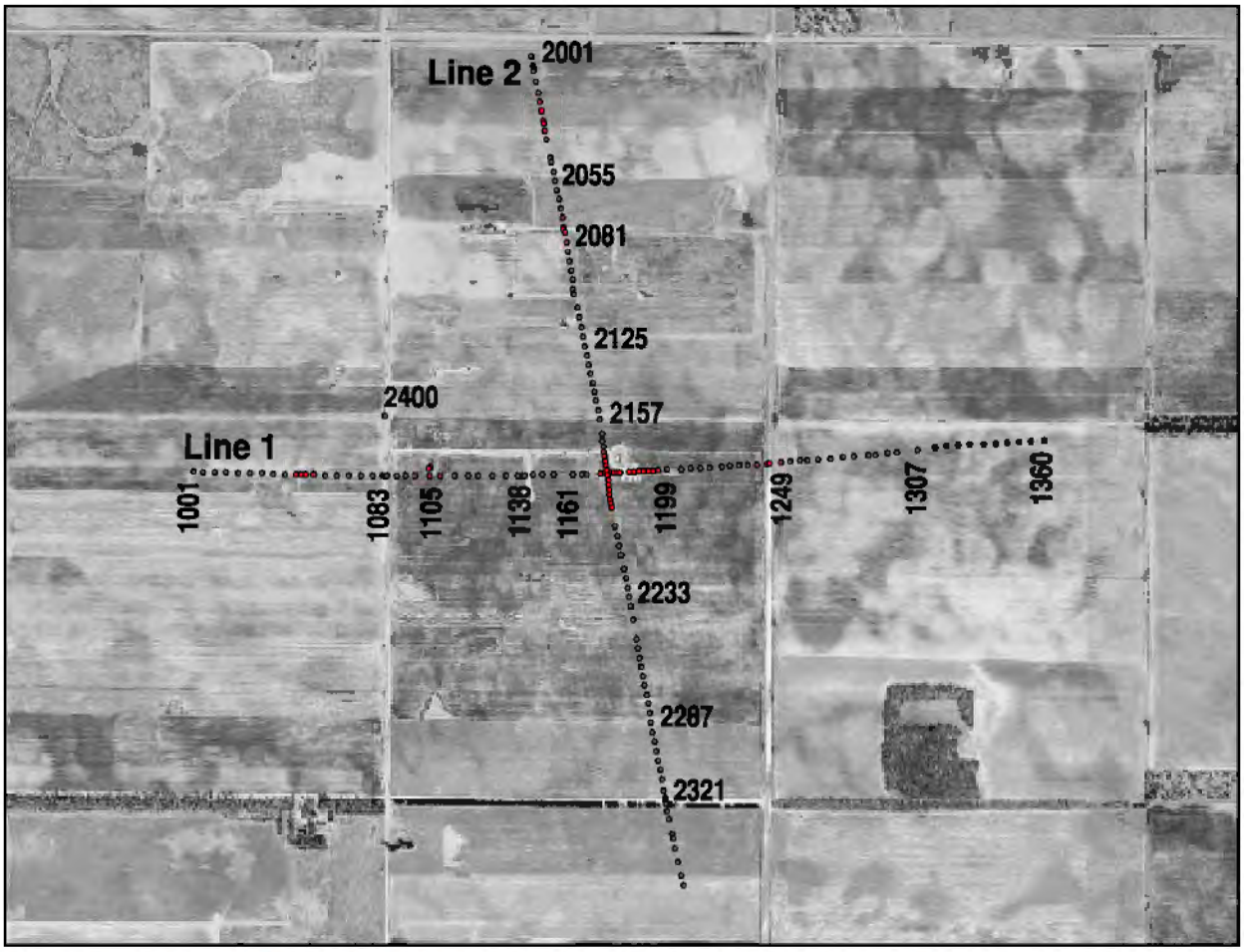

Figure 2. DGPS rtk (Differential Global Positioning System real-time kinematics) locations of lines 1 and 2 at the Leesburg sinkhole.

leaching of salt in Kansas possess an effective subsurface "root" or disturbed volume at least an order of magnitude greater in cross sectional area than the sinkhole itself. To avoid the sub-surface coverage shortfalls experienced by some previous seismic investigations of sinkholes in Kansas, this survey was designed to high-fold sample a 2-D subsurface slice 10 times the maximum diameter of the sinkhole.

Acquisition parameters were defined based on experience and walkaway tests along line 1. Twin Mark Products L28E 40Hz geophones were planted at 16-ft intervals in approximate 2-ft arrays. Geophones were planted into firm to hard soil in small divots left after the top few inches of loose material were removed to ensure good coupling. Four 60-channel Geometrics StrataView seismographs were networked to simultaneously record 240 channels of data. An IVI MinivibII using a prototype Atlas rotary servo valve delivered three 10-second, 20-250-Hz upsweeps at each shot location (shot interval was 16 ft). Experiments at this site were consistent with bench tests, which suggested this new rotary valve design will produce up to four times the peak force of conventional valves at 250 Hz. The pilot was telemetried from the vibrator to the seismograph and recorded as the first trace of each shot record. Each of the three sweeps generated per shot station was individually recorded and stored in an uncorrelated format with the ground force pilot occupying channel 1.

All sweeps were recorded into the fixed 240-channel spread with the source incrementally moved from shot station to shot station through the middle half of the spread. Once the center 120 receiver stations (60 shot stations) were shot through, the back 120 receiver stations were moved to the front and the process repeated. Because all shot records were recorded uncorrelated, QC involved visual inspection of the recorded pilot trace, audio monitoring of the pilot trace on a RF scanner, inspection of the vibrator power spectra after each shot, and review of a correlated shot record after every 5 to 10 shot stations. With the exception of receiver stations not instrumented due to excessive or thick gravel or asphalt or stations taken off-line when their offset exceeded 2000 ft, the survey was recorded with 98 percent live receivers within the optimum recording window (Hunter et al., 1984).

Reflections can be interpreted on raw, correlated shot records (scaled for display purposes) from around 30 ms to two-way time depths in excess of 800 ms. Considering the optimum window these data possess, it was imperative to keep a wide range of offsets to ensure the entire target zone was imaged. Reflections with dominant frequencies of around 200 Hz can be interpreted as deep as 200 ms, while the dominant frequency of reflections at 500 ms have dropped to around 100 Hz. Several milliseconds of reflection "chatter" observable between traces in proximity of the sinkhole is indicative of the dramatic localized changes in material velocities associated with rock layer failure and subsidence. Considering the dominant frequency of some reflections exceeds 200 Hz, a 2.5-ms static between adjacent traces represents a 180° phase shift and complete cancellation. Therefore, it is critical that these static irregularities be compensated for before the data are CMP stacked.

Seismic Processing

The basic CMP processing flow was consistent with 2-D high-resolution seismic-reflection methodologies (Steeples and Miller, 1990). All lines were processed using WinSeis2, beta seismic data-processing software (next generation of WinSeis Turbo) from the Kansas Geological Survey. Any reflection data acquired in this highly disturbed subsurface setting will be plagued with static problems and subject to dramatic swings in NMO velocity over relatively short distances; this data set was no exception. For the purposes of this survey, the surface topography was flat with the exception of the 10-ft-deep low associated with the 400-ft-wide sinkhole. Elevation data were acquired with an rtk DGPS (real-time kinematics Differential Global Positioning System) system with precision of less than 2 cm x, y, and z. Changes in velocity related to differentially compacted fill, anomalous rubble zones, and distorted rock layers produced several millisecond fluctuations in event arrival times across distances of 15 to 30 ft. In extreme cases, shifts of 10 ms can be measured across a span of less than 30 ft.

Data were recorded and stored uncorrelated to allow precorrelation processing in hopes of increasing the signal-to-noise ratio and resolution potential (Doll and Çoruh, 1995). Removal of noisy traces and amplitude scaling were precorrelation processing steps that significantly enhanced signal to noise and resolution potential. Attempts to improve the data quality precorrelation through frequency filtering, spectral whitening, and frequency-wave number (F-k) filtering were unsuccessful. Storing data uncorrelated also allowed tests to be run with different methods of correlation and correlating with different pilot traces. These data were optimally correlated using the synthetic drive signal. Storing data uncorrelated and unstacked required 30 times more storage space, about 50 percent more acquisition time, and 5 times more data transfer time. Improvements in signal-to-noise ratio and resolution made these increases cost effective.

Emphasis was placed on noise suppression, maintaining true amplitude, and compensating for velocity irregularities. Noise suppression focused on vehicle noise from the highway, livestock along the lines, powerline noise, surface waves, first arrivals, and air-coupled waves. Muting and hum filtering (Xia and Miller, 2000) improved signal-to-noise appreciably. The three individual shot gathers acquired at each shotpoint were vertically stacked after all the noise suppression operations were complete. With the exception of the 1-sec AGC used precorrelation and display gains, only spherical divergence was used to adjust trace amplitudes. With the large depth window of interest, a relatively wide optimum offset window was maintained, which after noise mutes resulted in true trace folds ranging from 1 to a maximum of 30 (Liberty and Knoll, 1998). Velocity was defined in groups of 20 CMPs with at least one control point for each 100-ms time window and a minimum of five points selected in the first 200 ms. Each line is defined by a velocity function with over 400 time/velocity pairs determined with the aid of several iterations of correlation static corrections and velocity analysis.

Even when reflections were interpretable within the noise cone, an inside mute was applied after the air-coupled wave to avoid signal degradation of reflection wavelets on CMP stacked sections. Inside mutes are a common practice for shallow (upper 3000 ft) seismic-reflection processing (Baker et al., 1998). It is however, uncommon and counterintuitive to remove confidently identifiable reflection events regardless of where they are relative to other energy arrivals. The likelihood of wavelet distortion sufficient to reduce the resolution potential or lose the trace-to-trace coherency of reflections is significantly increased when surgically muting noise immersed in signal. Analogous to inoperable tumors, attempts to precisely remove just noise—especially air-wave noise, at tolerances of a millisecond or two—runs the risk of cutting too severely and/or defining mute tapers that are too steep, thereby irreparably altering the reflection waveform. Stacking waveforms into the fold that have been distorted by overly aggressive mutes will compromise the accuracy of the information contained in the waveform, and in some cases produce artifacts that can be misinterpreted as true earth response.

Pump jack and wind noise were the two dominant noise sources. In both cases, careful muting during pre-correlation processing and pre-vertical stack/post correlation minimized the detrimental effects of noise on high-resolution low signal-to-noise data.

Seismic Interpretation

Confidently interpretable reflections on shot gathers are essential to optimizing the acquisition, processing, and interpretation of high-resolution seismic-reflection data. Dozens of reflections dominate the average shot gather from this site. Reflections throughout the primary time-depth target window (50 ms to 200 ms) possess broad spectral bandwidths and sufficient coherency to clearly interpret reflections across several to tens of traces. Reflection events can be traced through the air-coupled wave and just into the ground-roll wedge. To avoid any contamination by air-coupled wave, all energy after the airwave was removed during processing.

For quality control reasons it is important that reflections interpreted at two-way times less than 30 ms on CMP stacks can be correlated with equivalent 30-ms reflection hyperbolae on shot gathers. This consistency between shot records and stacked sections can be seen at various places along both lines of this survey. Identification of these reflections on field files and tracking of them throughout the processing flow was necessary to ensure CMP sections were correctly stacked and interpreted. Ultra shallow reflections (< 30 ms) were a critical aspect in discerning the periods since the Permian that these sediment-filled sinkholes may have been

active. Besides the reflection "chatter" indicative of lateral variations in material velocity, a striking characteristic of these seismic data is the contradictory AVO effects, depending on source and receiver orientation. Changes in reflection amplitude in this setting could be indicative of changes in acoustic impedance of the reflector itself and/or lateral variations in attenuation due to rock failure and collapse. True amplitude analysis intended to search for localized changes in material properties, possibly indicative of changes indicating increased loading, does not seem to be an effective first-order tool at this site.

Asymmetry of reflection hyperbolae observed in shot gathers across both lines results from dipping layers and velocity variability. Apparent shifts in the reflection apex are likely related to changes in velocity rather than dipping rock units when considering the scale of the distorted rock units relative to the spread length. Distortions of this kind will inhibit NMO velocity corrections that are based on the juxtaposition of first-order theoretical reflection hyperbolae with the moveout of actual reflections on CMP gathers. Many times these kinds of velocity irregularities are "removed" during processing by brute force adjustments using correlation statics techniques after best fit NMO corrections have been made. High-resolution delineation of bed offset is often easier and more accurate on shot gathers than CMP stacked sections. However, in the CMP domain this offset will be observed between adjacent CMPs, where it is evident between traces in the shot-gather domain. Faults that appear abrupt and definable within a few traces on shot gathers can appear smeared between several traces on CMP stacked sections, inhibiting interpretations that maximize the horizontal-resolution potential of these data. Reflections from the top of salt can experience 15 ms of difference at equivalent source offsets (less than 30 m) on opposite sides of the source.

CMP gathers hold the key to accurate representations of the subsurface on CMP stacked sections. Reflections after processing to adjust for non-vertical incidence, lateral variations in material velocity, and spherical attenuation of energy possess broad spectrum and consistent wavelets across the optimum offset range. The offset-dependent nature of frequency and amplitude characteristics are clearly evident in reflections deeper than 100 ms (~100 m). NMO velocities were defined for several of the primary reflecting interfaces to ensure minimum decay in frequency content after stacking.

High signal-to-noise ratio and bed resolution potential of observed reflections on shot and CMP gathers between about 80 ft and 2000 ft suffer little degradation as a result of horizontal stacking (Figures 3 and 4). Bed resolution on the order of 6 to 15 ft, depending on specific reflections, was more than sufficient for confident delineation of rock layers distorted by collapse into voids left after rock salt was leached away. Between the surface of bedrock and top of salt is an around-10000-ft-thick sequence of red-bed evaporites composed mostly of shales, sandstones, and anhydrites. The very plastic nature of these shale units is evident in the conformal nature of the bed geometries that overlies the highly altered layers of the salt unit. Amplitude changes across these fractured units are only interpreted in a very general fashion as related to compaction, bridging, and energy scattering. Dramatic subsidence structures revealed on CMP stacked sections allude to a complex chronology and non-linear relationship between multi-fluid source salt leaching and associated roof-rock failure.

Termination of the intra-salt reflections is likely related to the collapse of the less soluble anhydrite and shale units into voids left after dissolution of the salt. With the top of salt clearly evident as the high-amplitude reflection at about 320 ms, any bed distortions below about 400 ms are related to disturbances or nonlinearities in the wavefield that occur as energy travels through the layers disturbed by subsidence.

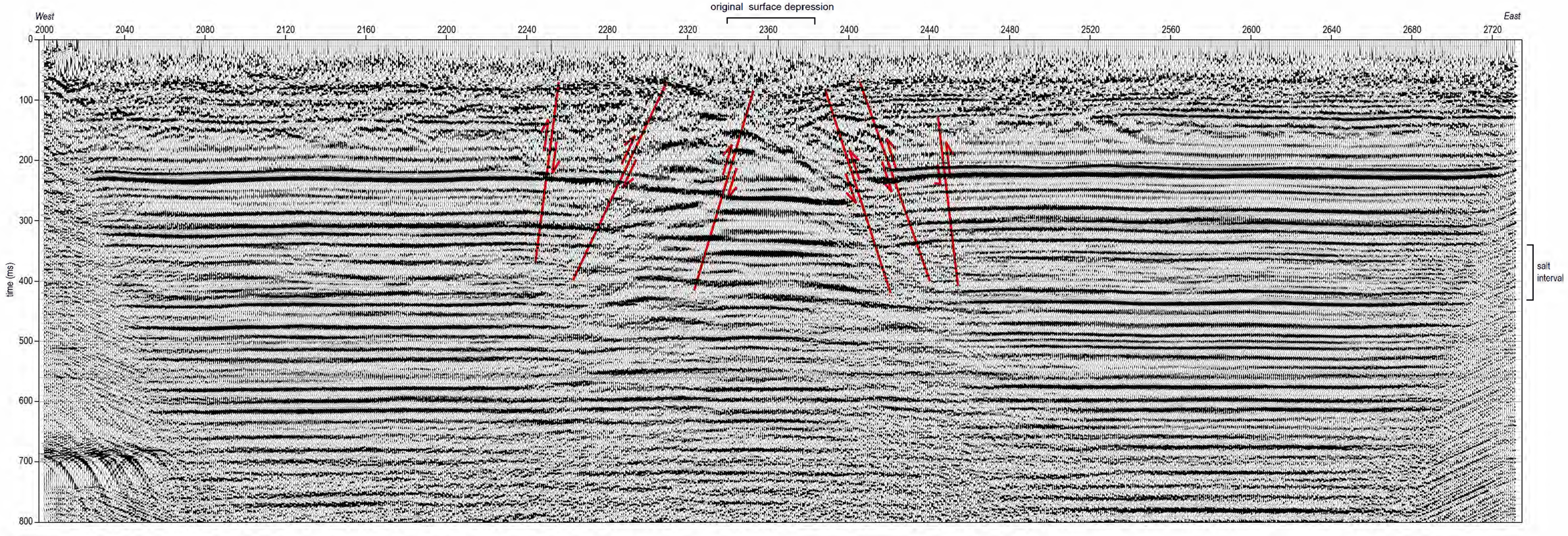

Figure 3. Leesburg line 1 with interpretation.

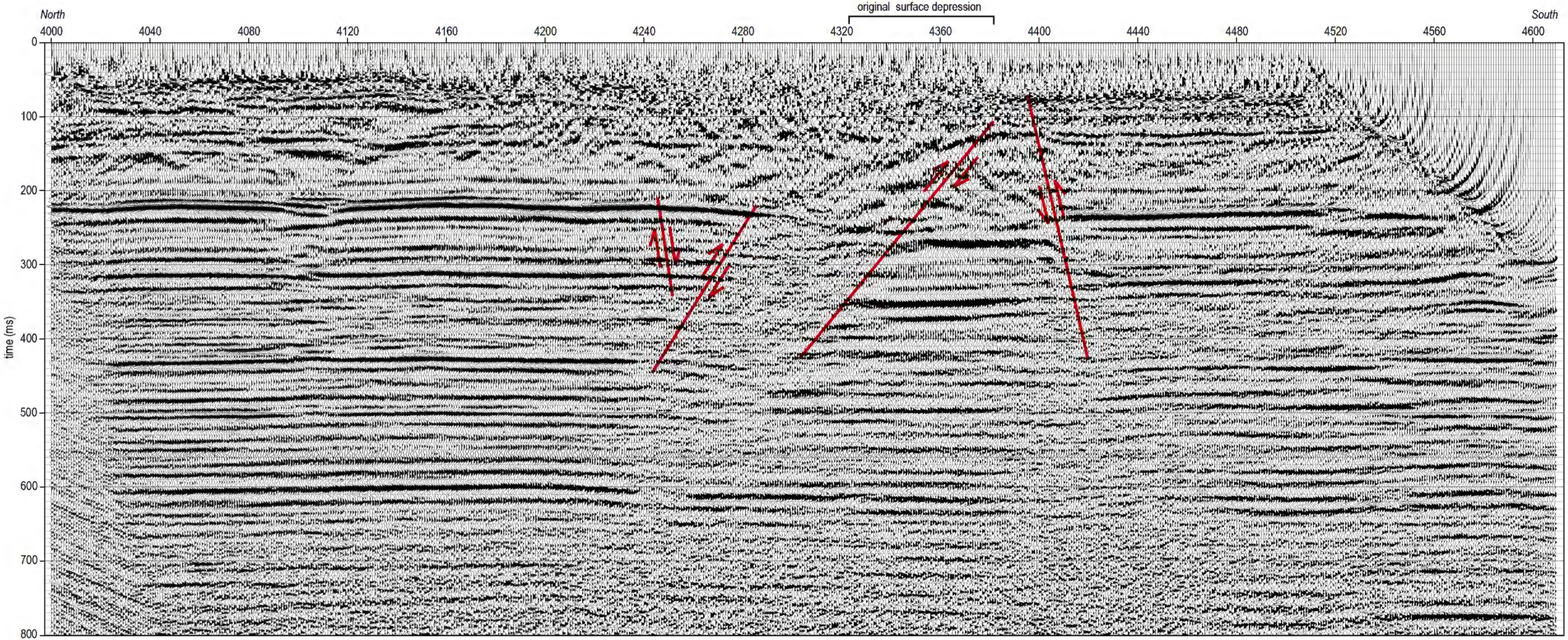

Figure 4. Leesburg line 2 with interpretation.

Within the zone measured as the current surface depression are several well-defined reverse and normal faults (Figures 3 and 4). These reverse faults are indicative of initial upward migration of dissolution voids with the roof rock being defined by a compressional stress regime. Once a sufficiently large collapse structure formed in the bedrock surface that the compressional stress could no longer be distributed around the opening in the chimney-like collapse structure that extended down to the salt layer, tensional stress began to dominate with normal faults indicative of the brittle deformation that followed and laterally extended the diameter of the sinkhole. The current sinkhole extends beyond the visible drape in the bedrock surface as a direct result of the movement of unconsolidated and saturated sediments above bedrock into the subsidence feature.

With the high-angle reverse fault defining the southern most extreme of the dissolution-induced subsidence, it is likely this is an area of active dissolution and a zone that has not yet transitioned from compressional to tensional stress. The change in stress regime must happen to return sediments above the salt to a relaxed state. Therefore, ground subsidence to the south should be expected in the future. Along the northern edge of the subsidence feature is a normal fault that clearly indicated that dissolution to the north has concluded and subsidence rates north should slow to stop in the future. When subsidence of the upper Wellington shales was or is controlled by compressional stresses, the rate of subsidence will be markedly more rapid and generally consistent with an upwardly narrowing cone defined by reverse faults. However, when the dissolution in a zone stops, the compressional forces give way to tensional stresses and the subsidence will gradually slow.

Several features are evident on these data away from the major dissolution feature that could be pertinent to future subsidence. On line 2 a significant disruption in the coherency of the reflection events is evident north of the sinkhole (Figure 4). This feature appears to originate in the salt and expand upward. This kind of geometry is not consistent with dissolution-induced sinkhole development. In the worst case, the angle of draw should not exceed about 15% in this setting, with initial failure being along reverse faults. That means that the dissolution void had to have been wide enough to promote roof failure. This feature deserves more study.

West of the subsidence related to the sinkhole are obvious undulations in the Stone Corral anhydrite that are not static and appear related to dissolution along the contact between the salt and overlying shales (Figure 3). This feature could be indicative of a zone that might be more susceptible to dissolution (previous access to freshwater and fluid exit). These subtle synclines are obviously pre-anthropogenic and therefore unlikely to represent a threat to surface stability.

Discussion

Reflections in proximity to and beneath the sinkhole were highly distorted with a collapse structure well defined in the subsurface. Subsidence geometry of the 220-ms-deep Stone Corral Formation is unique compared to previously studied single-well sinkholes where salt was at a similar depth and dissolution was instigated by oil-field well-casing failure. At this site it appears the Stone Corral Formation failed as large, relatively intact blocks with the largest segment measuring around 500 ft to 700 ft in length and down-dropped around 150 ft (after compensation for the reduced average velocity within the disturbed near-surface) located immediately beneath the sinkhole. Other large pieces of this anhydrite layer appear to have tilted in response to progressive leaching of the salt and expansion of the dissolution front.

Interpreted bed offset geometry/orientation is unique to this subsidence feature and provides important clues to possible growth mechanisms. Faults interpreted as defining layer displacement resulting from failure are different on one side of the subsidence feature relative to the other. As with all other subsidence features, opposing reverse faults clearly define the initial failure cone and are centered on the current sinkhole at about CMP 2360. Based on surface-elevation data, the most rapid vertical growth is along the eastern side of the sinkhole, while very little vertical growth has been observed to the west; the sinkhole clearly possesses a very gentle ground surface slope toward the sinkhole center from all directions.

It is reasonable to correlate future surface growth with the unique reflection geometries on opposing sides of this subsidence feature. Gradual expansion in the radius of the sinkhole to the west is consistent with normal-fault offset geometries in bedding as would be anticipated during gradual relaxation of the accumulated stress after salt leaching has ceased. The predominantly vertical growth evident throughout this structure is interpreted to correlate with subsurface sediments that are subsiding along reverse-fault planes during initial formation. The asymmetry in rock geometries apparent within the overburden on seismic images is a bit unusual for a single borehole-induced dissolution void. Future surface growth will likely correlate with this non-linear radial-growth pattern observable in the subsidence-altered reflections beneath the sinkhole.

Unique to this sinkhole is the multi-well hydrologic system and the nonsymmetrical reflection and bed-offset geometries about the principal well bore. It is likely these two unusual situations/characteristics are cause and effect, respectively. This lack of verticality, normally observed in well-induced subsidence features, is also a likely result of this two-well system. The hydrostatic head of the completion units (geologic) for each well would dictate fluid-flow direction (artesian or gravity) and volumes. With the enhanced potential for fluid transport, this two-well system could eventually lead to leached volumes and a subsequent sinkhole significantly larger than any single-well sinkhole currently known to exist.

Careful study of geometries prevalent in this seismic image provides important clues to sinkhole growth and factors influencing areas of active leaching. Bed offsets on the east are markedly different in orientation and general geometry relative to the west side of the structure. Building on the observations on seismic-reflection surveys at other subsidence sites, the more reverse-fault-dominated east side of the structure is likely to support the majority of future subsidence. Implications from previous sites would support the suggestion that normal-fault-controlled subsidence on the west is the response to gradual relaxation of stress over an area without current leaching. On the east, however, the reverse-fault architecture bounding the outermost perimeter of the subsidence volume is one indicator of active leaching and potentially higher subsidence rates resulting in a much larger surface expression.

Conclusions

High-resolution seismic-reflection profiles acquired at the Leesburg sinkhole in Stafford County, Kansas, during July 2004 imaged geologic features indicative of dissolution in the Permian Hutchinson Salt Member at a depth beginning around 800 ft to as much as 1200 ft below ground surface. Subsurface subsidence and bed distortion associated with the sinkhole is currently around 1600 ft in diameter and skewed slightly north and west of the sinkhole. Based on the bed geometries and apparent offset features with normal fault characteristics in the upper 1200 ft below ground surface, gradual subsidence is likely to continue, predominantly in an eastern and southern direction.

South and east extremes of the subsurface subsidence are marked by very abrupt offset features with apparent reverse-fault geometry. It is generally thought that subsidence marked by reverse-fault geometry is related to the initial movement of rock layers prior to surface expression. Active dissolution will be marked by reverse faults in the overburden that bound the subsidence area.

West of the surface depression are two very pronounced features with synclinal geometry extending into the interval interpreted as the salt. These synclinal features are indicative of dissolution and resulting subsidence of overlying Permian strata, predominantly shale sediments.

North of the sinkhole is a feature that appears to originate in the salt and intensify upward in the magnitude of rock distortion. This feature is asymmetric and did not have an obvious surface expression at the time of the survey. With no other information except these 2-D seismic sections, this area is about a quarter-mile north of the sinkhole and justifies attention.

These seismic data are of very good to excellent quality and provide very clear evidence that the surface depression is directly related to dissolution of the salt beneath several well sites. Based on the apparent subsurface expression and areas within the salt where dissolution appears to have been or is active, this sinkhole will likely grow to over a quarter-mile in diameter with a potential footprint as much as a half-mile in diameter.

References

Anderson, N.L., R.W. Knapp, D.W. Steeples, and R.D. Miller, 1995b, Plastic deformation and dissolution of the Hutchinson Salt Member in Kansas: Kansas Geological Survey Bulletin 237, p. 66-70.

Anderson, N.L., W.L. Watney, P.A. Macfarlane, and R.W. Knapp, 1995a, Seismic signature of the Hutchinson salt and associated dissolution features: Kansas Geological Survey Bulletin 237, p. 57-65.

Anderson, N.L., A. Martinez, and J.F. Hopkins, 1998, Salt dissolution and surface subsidence in central Kansas: A seismic investigation of the anthropogenic and natural origin models: Geophysics, v. 63, p. 366-378.

Baar, C.A., 1977, Applied salt-rock mechanics 1: Elsevier Scientific Publishing Company, 294 p.

Baker, G.S., D.W. Steeples, and M. Drake, 1998, Muting the noise cone in near-surface reflection data: An example from southeastern Kansas: Geophysics, v. 63, p. 1332-1338.

Bayne, C.K., 1956, Geology and ground-water resources of Reno County, Kansas: Kansas Geological Survey Bulletin 120.

Beck, B.F., A.J. Pettit, and J.G. Herring, eds., 1999, Hydrogeology and engineering geology of sinkholes and karst–1999: A.A. Balkema.

Carter, N.L., and F.D. Hansen, 1983, Creep of rock salt: Tectonophysics, v. 92, p. 275-333.

Davies, W.E., 1951, Mechanics of cavern breakdown: National Speleological Society, v. 13, p. 6-43.

Doll, W.E., and C. Çoruh, 1995, Spectral whitening of impulsive and swept-source shallow seismic data [Exp. Abs.]: Society of Exploration Geophysicists, p. 398-401.

Ege, J.R., 1984, Formation of solution-suhsidence sinkholes above salt beds: U.S. Geological Survey Circular 897, 11 p.

Frye, J.C., 1950, Origin of Kansas Great Plains depressions: Kansas Geological Survey Bulletin 86, pt. 1, p. 1-20.

Frye, J.C., and S.L. Schoff, 1942, Deep-seated solution in the Meade Basin and vicinity, Kansas and Oklahoma: American Geophysical Union Transactions, v. 23, pt. 1, p. 35-39.

Hunter, J.A., S.E. Pullan, R.A. Burns, R.M. Gagne, and R.S. Good, 1984, Shallow seismic-reflection mapping of the overburden-bedrock interface with the engineering seismograph–Some simple techniques: Geophysics, v. 49, p. 1381-1385.

Knapp, R.W., D.W. Steeples, R.D. Miller, and C.D. McElwee, 1989, Seismic reflection surveys at sinkholes in central Kansas; *in*, Geophysics in Kansas, D.W Steeples, ed.: Kansas Geological Survey Bulletin 226, p. 95-116.

Liberty, L.M., and M. Knoll, 1998, Time varying fold in high-resolution seismic reflection data: a recipe for optimized acquisition and quality control processing and interpretation: Proceedings of the Symposium on the Application of Geophysics to Engineering and Environmental Problems (SAGEEP 98), Chicago, Illinois, March 22-26, p. 745-751.

Merriam, D.F., and C.J. Mann, 1957, Sinkholes and related geologic features in Kansas: Transactions Kansas Academy of Science, v. 60, p. 207-243.

Miller, R.D., D.W. Steeples, L. Schulte, and J. Davenport, 1993, Shallow seismic reflection study of a salt dissolution well field near Hutchinson, Kansas: Mining Engineering, October, p. 1291-1296.

Miller, R.D., D.W. Steeples, and T.V. Weis, 1995, Shallow seismic-reflection study of a salt-dissolution subsidence feature in Stafford County, Kansas; *in*, Geophysical Atlas of Selected Oil and Gas Fields in Kansas, N.L. Anderson and D.E. Hedke, eds.: Kansas Geological Survey Bulletin 237, p. 71-76.

Miller, R.D., A.C. Villella, and J. Xia, 1997, Shallow high-resolution seismic reflection to delineate upper 400 m around a collapse feature in central Kansas: Environmental Geosciences, v. 4, n. 3, p. 119-126.

Rokar, R.B., and K. Staudtmeister, 1985, Creep rupture criteria for rock salt; *in*, Sixth International Symposium on Salt, B.C. Schreiber and H.L. Harner, eds.: Salt Institute Inc., Virginia, v. 1, p. 455-462.

Steeples, D.W., and Miller, R.D., 1990, Seismic reflection methods applied to engineering, environmental, and groundwater problems; *in* Geotechnical and Environmental Geophysics, Vol. 1: Review and Tutorial, Stan Ward, ed., Society of Exploration Geophysicists, p. 1-30.

Steeples, D.W., R.W. Knapp, and C.D. McElwee, 1986, Seismic reflection investigation of sinkholes beneath interstate highway 70 in Kansas: Geophysics, v. 51, p. 295-301.

Walters, R.F., 1978, Land subsidence in central Kansas related to salt dissolution: Kansas Geological Survey Bulletin 214, p. 1-32.

Walters, R.F., 1980, Solution and collapse features in the salt near Hutchinson, Kansas: South-central Section, Geological Society of America, Field Trip Notes, 10 p.

Walters, R.F., 1991, Gorham oil field: Kansas Geological Survey Bulletin 228, p. 1-112.

Watney, W.L., J.A. Berg, and S. Paul, 1988, Origin and distribution of the Hutchinson salt (lower Leonardian) in Kansas: Midcontinent SEPM Special Puhlication No. 1., p. 113-135.

Xia and Miller, 2000, Design of a hum filter for suppressing power-line noise in seismic data: Journal of Environmental and Engineering Geophysics, v. 5, n. 2, p. 31-38.

Appendix

SEISMIC INVESTIGATIONS OF SUBSIDENCE FEATURES IN KANSAS

Introduction

High-resolution seismic-reflection surveys targeting the Hutchinson Salt Member have collectively provided critical insights and valuable site-specific characteristics of subsidence features throughout Kansas. Significant findings from these various studies are collectively applicable to any region underlain by massive bedded salt layers and in general to any collapse processes in a subsidence-prone setting. A high concentration of seismic profiles has been collected along the natural dissolution front and specific dissolution mine fields where subsidence has threatened transportation and/or population centers. This concentrated area of study in conjunction with several sinkhole investigations scattered around the central part of the state of Kansas allow empirical development of mechanisms and settings controlling and influencing the subsidence process (Figure 1).

A range of sinkhole types and locations has been seismically investigated en route to addressing site-specific questions generally related to prediction of future growth rates and affected surface. In part, as a consequence of these focused studies, the high-resolution seismic-reflection method has been refined and, therefore, evolved over the last 15 years to more effectively and accurately image extreme structural anomalies. Sinkholes included in these various studies have formed as a result of salt dissolution both in proximity to well bores (dissolution mining, brine disposal, oil wells, seismic shot holes, etc.) and in areas known to experience natural dissolution with no apparent anthropogenic influences. The eastern boundary of the salt is a natural leaching environment where sinkholes have been forming for millions of years and is significantly less predictable and potentially controllable than subsidence resulting from anthropogenic fluid sources.

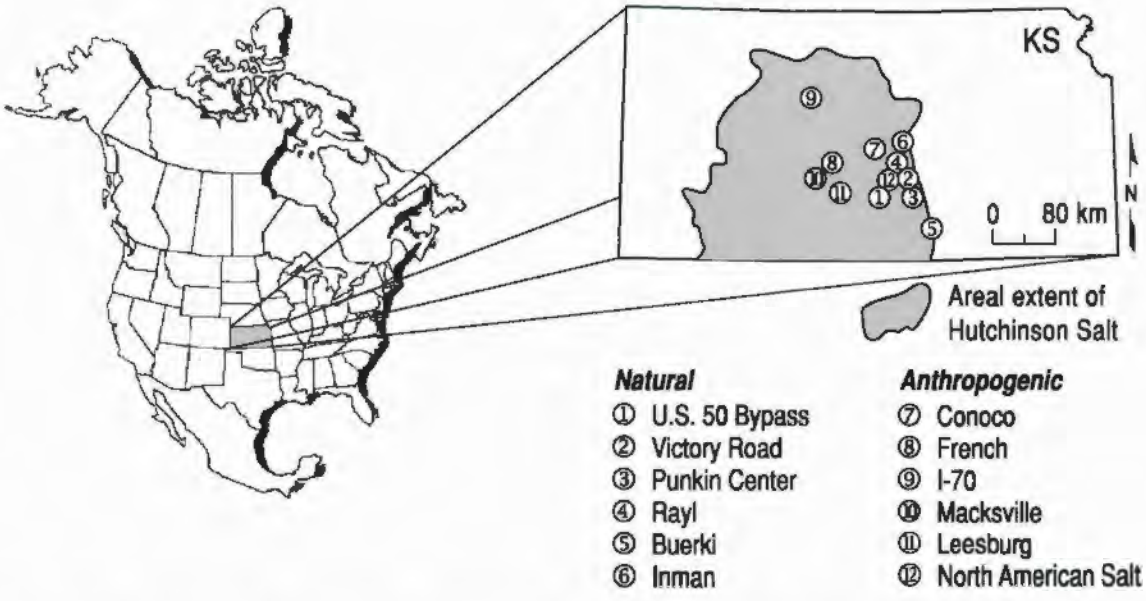

Figure 1. Map of Kansas with outline of areal extent of Hutchinson Salt Member. Numerically identified on the map are locations of 12 high-resolution seismic-reflection surveys targeting individual sinkholes. These sites include over 60 km of high-resolution seismic data on 28 different lines, all acquired, processed, and interpreted by or under the direction of the author.

Each seismic-reflection study targeting the Hutchinson salt bed and shallower layers where subsidence was a possibility or has been observed produced seismic images of legacy or active dissolution features generally possessing consistent characteristics and geometries. Twelve seismic investigations originally and individually designed to search for clues amenable to predicting ground stability and associated future sinkhole(s) collectively provide a unique opportunity for joint interpretations in support of a more regional subsidence study with overtones significant to collapse structures worldwide. When considering the limited number of seismic-reflection surveys specifically designed to delineate collapse structures associated with salt dissolution, it is not surprising that unique scientific contributions can be extracted for every seismic image in this set of 12. Upcoming discussions segregate these 12 subsidence features into anthropogenic and natural (Table 1), with the unique characteristics of each described and then assimilated into a collected set of findings for inclusion in an empirical subsidence model.

Seismic Investigations of Natural-dissolution Subsidence

Several natural-dissolution features were discovered as a result of a 10-km seismic-reflection investigation along a proposed highway expansion approximately 20 km west of the Hutchinson Salt Member's natural-dissolution front (Table 1 ①). Many of these dissolution features possess characteristics indicative of different stages of development and duration and number of solution episodes. One paleosubsidence feature imaged during this survey that is of particular interest possesses a very well defined subsidence geometry characteristic of both rapid initial compressional subsidence and the commonly observed broad tensional bowl-shaped feature (Figure 2). This distinctive 300-m-wide paleosubsidence feature has no current surface expression and was totally unexpected this far from the natural-dissolution front.

Breaking down this seismic image of a paleosinkhole beyond its two principal subsidence components reveals a variety of unique attributes. This is one of the few known natural dissolution features this far (15 km) from the dissolution front that is not related to regional faulting (Walters, 1980). An increased reflection amplitude along the salt/shale caprock interface (~160 ms) and highly disturbed area in the salt at the apex (trough) (~CMP 1870) of the subsurface synform are both characteristics indicative of subsidence due to dissolution near the

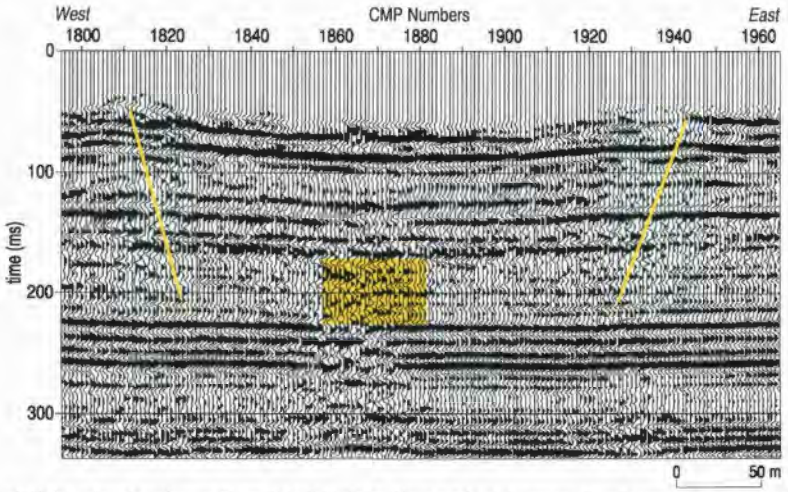

Figure 2. A portion of this stacked section highlights the subsidence-feature geometry. The box includes what is interpreted as a dissolution volume, seismic unique with diffractions from bed terminations and low-frequency, more chaotic events.

Table 1. Unique and Specific Characteristics of Each Study

NATURAL

Site Name	Parameters		Goal	Scientific Contribution
	Acquisition	Processing		
① U.S. 50 Bypass	19-bit A/D 240 channels 2.5-m receiver 5-m source Vibrator	Spectral balance Gross velocity Severely reduced fold (12-14)	No sinkholes, but search for anomalies above and within salt that might represent collapse risks for proposed highway.	Non-vertical subsidence growth, single episode collapse with central chimney and oversized bowl in near surface (Miller, 2003).
② Victory Road	19-bit A/D 240 channels 2.5-m receiver 5-m source Vibrator	Spectral balance Severe mute NMO velocity Sub-spread static ¼ λ	Recent sinkhole affecting major highway, predict growth and rate and safety for filling.	Dual stress regimes obvious, but multiple reactivations make unraveling complete history impossible. Sinkhole part of larger system (Miller, 2006).
③ Punkin Center	16-bit A/D 48 channels 2.5-m receiver 2.5-m source 8-gauge auger gun	10 CMP velocity Iterative ¼ λ statics Time-variable bandpass Heavy mute	Determine relationship between oil field and sinkhole in area with multiple natural sinkholes.	Paleosinkholes with steep-sided chimney within an area characterized by dissolution-induced undulating overburden.
④ Rayl	19-bit A/D 240 channels 2.5-m receiver 5-m source Vibrator	NMO velocity Static iteration Severe mute Spectral balance Subspread in sink	Predict sinkhole growth and establish if oil well in portion of sinkhole responsible for dissolution casing subsidence.	Multiple previous episodes of dissolution and paleo-subsidence with well asymmetric to dissolution. Complex interfingering.
⑤ Buerki	12-bit A/D 24 channels 2.5-m receiver 2.5-m source 50-cal.	Low-cut filter Detailed noise removal Low-fold overburden	Determine if sinkhole was natural or anthropogenic.	Irregular subsidence pattern proposed to be inconsistent with point-source leaching.
⑥ Inman	19-bit A/D 240 channels 2.5-m receiver 5-m source Vibrator	NMO velocity every CMP Severe mute Spectral balance No vertical stack	No confirmed sinkhole where highway crossing dissolution front. Investigate and delineate any dissolution structures.	Bridging interpreted based on amplitude characteristics, abrupt nature of front not evident at surface.

Table 1 (continued)

ANTHROPOGENIC

Site Name	Parameters		Goal	Scientific Contribution
	Acquisition	Processing		
⑦ Conoco	12-bit A/D 24 channels 16-m receiver 16-m source MiniSosie	NMO every 10 CMP Minimum fold processing No wavelet Iterative statics Large CORR window	Predict growth; specifically, potential effect on road and farm house.	Bowl-shaped depression above salt interpreted normal at time, later clearly reverse and normal faults (Miller et al., 1985).
⑧ French	19-bit A/D 96 and 120 channels 5-m receiver 5-m source Vibrator	Velocity function highly detailed Static w/multiple replacement velocities Multiple statics iterations	Evaluate failure potential of ground inside sinkhole for plugging operations. Predict growth rate and extent of sinkhole.	First dual-stress field sinkhole with confidently interpretable reverse and normal faults that match physical models (Miller et al., 1997).
⑨ I-70	19-bit A/D 240 channels 5-m receiver 16-m source Vibrator	Spatial variable CMP High-density velocity Spatial variable mute–compressed CMP spread	Evaluate dissolution change and estimate growth potential and rapid subsidence risk.	Majority reverse with minor normal matching physical models for active dissolution beyond surface collapse (Miller et al., 2006).
⑩ Macksville	19-bit A/D 240 channels 5-m receiver 10-m source Vibrator	Detailed NMO velocity Reduced trace count to option Heavy mute	Establish growth characteristics of sinkhole and unique properties of catastrophic initial failure that is currently gradual.	Active subsidence areas associated with dissolution move laterally, generally in a reverse fault geometry at the active face (Lambrecht and Miller, 2006).
⑪ Leesburg	19-bit A/D 240 channels 5-m receiver 16-m source Vibrator	Migration filter Time-variable filter Spectral balance High kill to balance trace window	Predict future surface growth and develop concept related to apparent multi-well involvement.	Most geometrically distorted feature with extensive subsurface expression relative to surface—first multi-source anthropogenic dissolution features.
⑫ North American Salt	12-bit A/D 24 channels 2.5-m receiver 2.5-m source Downhole 50-cal.	Tight bandpass Severe muting Minimal fold Detailed NMO High stretch mute	Determine potential and extent of future subsidence, especially beneath road and railroad.	Delineated collapse roof halted within dome, roof material tensional under dome, dome undisturbed (Miller et al, 1993).

salt/caprock contact and collapse breccia within the entire salt volume near the center of the subsidence, both diagnostic of an ancient dissolution feature. Because natural dissolution has a greater tendency to occur along the impermeable and insoluble caprock or at the base of interbedded layers within the salt, the relatively vertical volumetric representation of dissolution at the center of the subsidence feature seems unusual (Figure 2). Diffractions within the altered salt volume are consistent and generally synonymous with irregular features or layer discontinuities such as voids, faults, or bed terminations.

The apparent vertical elongation of this paleodissolution feature within the salt interval is unusual and likely due to the presence of localized fractures oblique to the orientation of the seismic line. No seismic evidence to support faulting as a possible conduit for fluid migration at this location is known. Any discontinuity in the subsalt layer could have acted as a thoroughfare for ground water to access the salt interval. Considering the increase in fluid density with increased salinity, one possible explanation for this localized leached volume is the migration of unsaturated fluids vertically from the base of the salt interval through the salt and expansion along the salt and overlying shale contact (morning-glory structure). With the interbedded nature of the salt, individual solution voids must have grown to the point they were large enough at the base of each interbedded shale and anhydrite layer to precipitate failure, thereby creating the pathway necessary to accommodate vertical fluid migration and eventual development of this disturbed salt volume. Alternately, because these interbedded layers are known not to be laterally continuous over a distance more than a few kilometers, this volume could be consistent with the coincident termination of several interbedded units.

It appears from the seismic image that once fluid contacted the massive insoluble shale caprock, leaching was constrained and guided along this contact. Vertical migration was halted at the base of the shale caprock and the dissolution front began spreading radially from the disturbed salt volume at the center of the present synclinal feature. Gradual and incremental subsidence continued until the leaching process ended, leaving the collapse structure as interpreted on the seismic section extending from CMPs 1820 to 1940 (~300 m). At this point, the hydrodynamics of this feature apparently changed and the dissolution and subsidence process appears to have at least temporarily ended.

Seismic characteristics of the draping beds and intersalt disturbances are key to and help build the foundation for suggestions concerning the dissolution and collapse history of this feature. Reflections immediately below the salt interval possess a distinctive velocity or static pull-down relative to undisturbed rock on either side. This pull-down is due to the reduced overburden velocity within the subsidence-affected area. Significant to the validity of this interpretation are the very well shaped and relatively undisturbed diffraction events originating from within the salt and predominantly near the apex of the subsidence synform. Also noteworthy with respect to the top of salt reflection is the decrease in dominant frequency. Wavelet changes associated with the top of the salt within this dissolution feature are consistent with theoretical developments for void/rubble replacement of competent rock beneath a caprock.

An alternative interpretation of fluid migration critical to development of this dissolution feature puts the inlet or source within the overburden. If fluid entered from above the salt, dissolution would have also preferentially occurred near the top, expanding along the insoluble caprock, consistent with the location of the fluid outlet. Considering the predominantly vertical dissolution volume interpreted on seismic data from within the salt, fluid exiting through the salt and into the substrata would have been heavily laden with salt, likely fully saturated, thereby leaching within the salt would have been minimal. Saturated fluid moving through the salt

would not enlarge the dissolution volume. Critical to this fluid movement scenario is the clear passage through the salt. Because this feature is natural and likely structurally controlled, the three-dimensional aspects of the fluid conduit must also be considered, making fractures a potential controlling influence.

This single-episode subsidence feature is interpreted to be an example of the initial stage in the maturation of a natural dissolution-induced subsidence feature. Multiple-episode subsidence structures that have been seismically imaged possess significantly more complex reflection geometries and are influenced by numerous reactivations of leaching, generally followed by periods of dormancy and/or continued leaching through newly established localized fluid pathways. These multi-episodal superstructures can be kilometers in diameter and active throughout an extensive period of leaching with a multitude of distinct voids in various stages of migration toward the ground surface.

A study designed to investigate the subsurface beneath a 100-m-wide sinkhole near the natural dissolution front uncovered one of these massive subsidence features without surface expression and acting as the parent structure to the small active sinkhole targeted by this particular investigation (Table 1 ②). High signal-to-noise ratio and high-resolution seismic-reflection data allowed detection, delineation, and evaluation of rock failure associated with multiple episodes of material collapse after periodic and localized natural leaching of the 125-m-deep, 40-m-thick Permian Hutchinson Salt Member (Figure 3). Mechanisms and gross chronology of structural failures as interpretable from stacked seismic sections were principally influenced by pre-Pliocene-Pleistocene to current dissolution. Dating the structural progression of this entire feature is in part based on the relatively flat appearance of shallow reflections above highly altered rock; this observation implies subsurface stability since deposition of the shallowest Quaternary material.

Collapse of the consolidated overburden sediments (predominantly shale) responsible for the currently active sinkhole appears to have been strongly influenced by the maximum stress lines associated with the tensional dome model. As leaching continued, the radius of failure

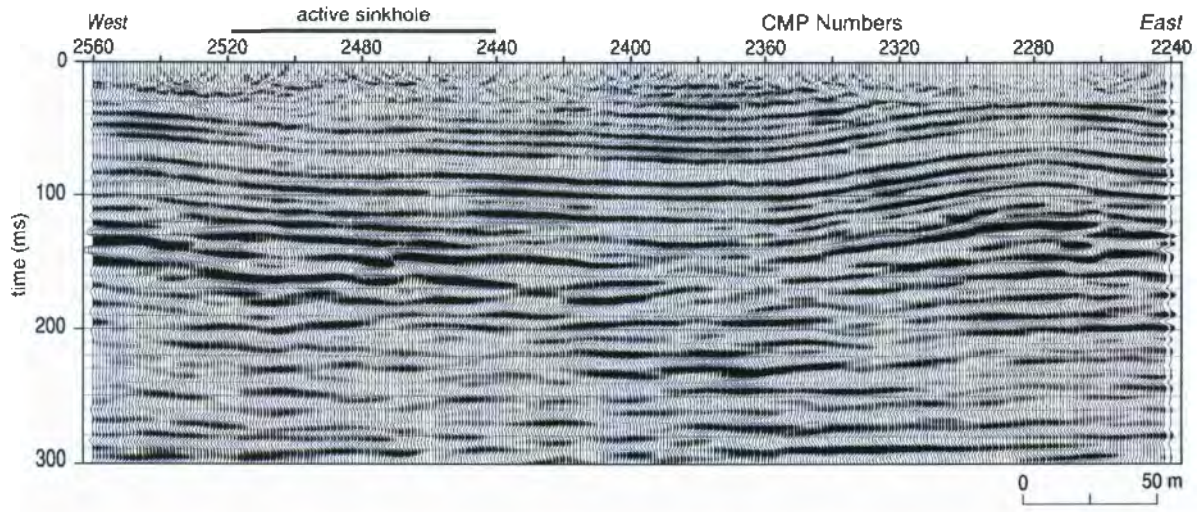

Figure 3. Migrated nominal 60-fold CMP stacked section crossing a 100-m-wide surface depression centered on station 2480. The Hutchinson Salt Member interval has been correlated with nearby borehole logs and is between 120 ms and 160 ms two-way traveltime. With no surface expression except the 100-m-wide sinkhole at 2480, it is reasonable to interpret a paleosubsidence feature that is at least 400 m wide.

progressively increased with subsidence predominantly controlled or at least defined by concentric sets of reverse-fault geometries interpreted from offset in overburden rock layers (Figure 4). This series of sub-parallel reverse-fault planes geometrically matches the lines of stress that would define the initial failure tensional dome. At least two distinct episodes of collapse along groupings of reverse faults define this active subsidence structure, with the beginnings of a third and likely final collapse phase indicated by normal faults at the extreme outside of this feature. Enlargement of the collapsed overburden volume appears to have progressed in this fashion with several periods of dissolution at each of several smaller structures across this massive large-scale structure.

Once the salt-void growth ended and so the undercutting of competent overburden along the perimeter of the dissolution volume also ended, overhanging layers or ledges of rock (hanging wall) were left under significant extensional stress. These ledges extend around the perimeter of the cone/chimney structure supporting an upward-thickening, relatively undisturbed volume of rock through the upper Permian section. Relative movement of rock layers around the outer portion of the subsidence feature is interpreted to have been influenced by faults with normal orientations or geometries. This suggests the stress environment in and around this subsidence feature took on more extensional characteristics at this point. Hence, after dissolution concluded, downward movement (settling, relaxation) of sediments around the perimeter of the initial subsidence volume appears to have been driven by gravity and controlled/influenced by weakened rock layers above and on the perimeter of the dissolution zone.

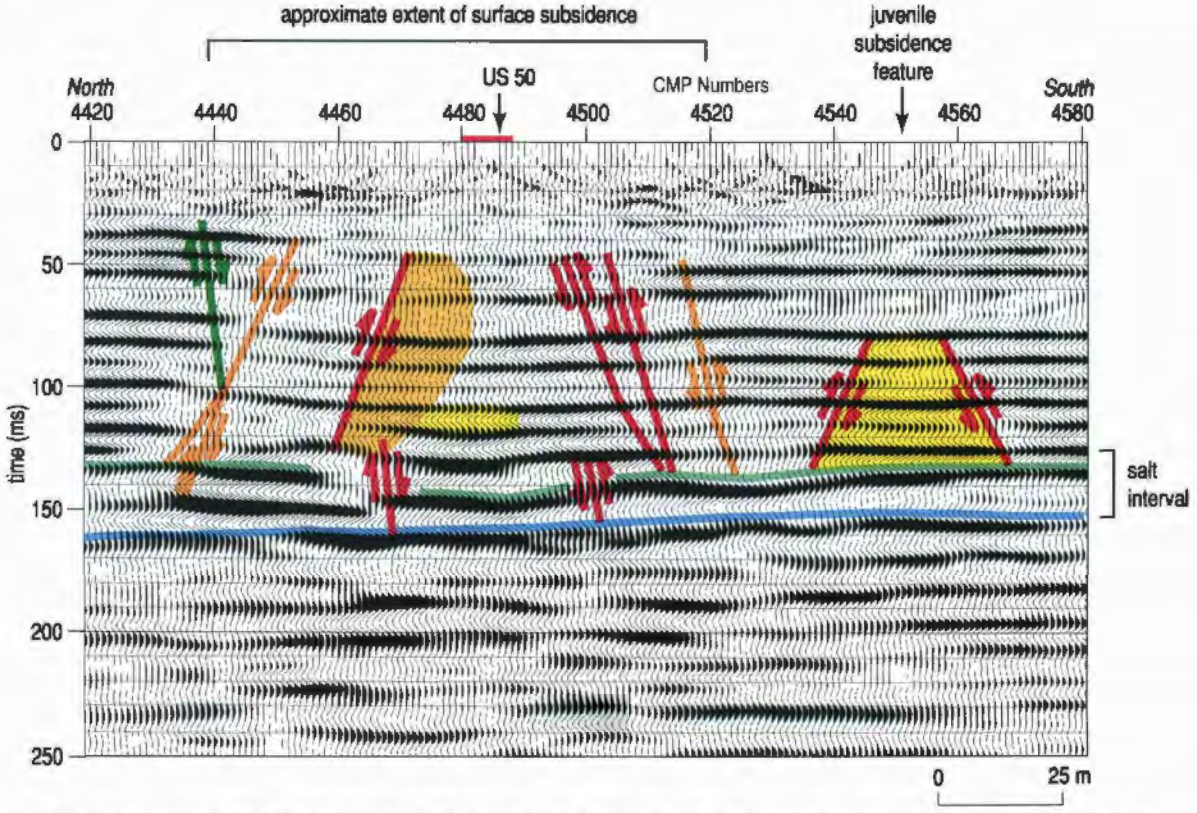

Figure 4. Interpreted CMP stacked section with disturbed salt interval at about 120 ms to 160 ms two-way traveltime. Several possible interpretations would be valid for this migrated section. Of particular interest is the small juvenile subsidence feature interpreted beneath station 4550 about 70 ms deep. Red bar near 4480 is location of highway crossing line at nearly a right angle.

With the termination of salt-void growth, little or no incremental accumulation of stress occurred and gradual subsidence continued advancing radially as an ever-expanding bowl (synform), geometrically defined by normal-fault planes. Based on the reflection geometries, expansion beyond the perimeter defined by the edges of the dissolved salt and associated reverse-fault planes has resulted from extensional stress, gravity slumping, and differential compaction of the solution void that was at least partially filled with collapse breccia during initial failure. Normal-fault geometries define a bowl-shaped structure near the perimeter of the collapse feature while a series of upward-narrowing cones defined by the reverse-fault planes are evident near the center of the subsidence feature. This sequence of events both explains and is consistent with the rock geometries defined by these seismic data and known geology.

Captured on these seismic data is what has been interpreted as a juvenile subsidence feature (Figure 4). Beneath CMP station 4550 there appears to be a subsidence feature with subtle drape in the 80-ms reflection and a triangular shape (on this 2-D section) defined by relative bed offsets consistent with reverse faults. This fault geometry was previously described as characteristic of initial roof failure of a void with reverse-fault planes equated to lines of equivalent stress above an unsupported span of roof rock. One of the keys to this postulated juvenile subsidence feature is the slight increase in amplitude of and time delay in the shallowest salt reflection, characteristics interpreted to be consistent with dissolution along an acoustic-impedance contrast (reflector). It is not clear whether this subsidence is active or dormant, but it does seem to be a likely location for future subsidence along this profile.

As seen on the previous data set from U.S. 50 Highway, this profile also inadvertently crossed a paleosubsidence feature (Figure 5). This seismic profile provides dramatic evidence supporting the seismically inferred failure processes and resulting bed geometries. At the eastern extreme of this buried collapse structure is an abrupt and intact reverse fault interpreted above the salt interval and bounding the eastern edge of the synform. On the western extreme of the

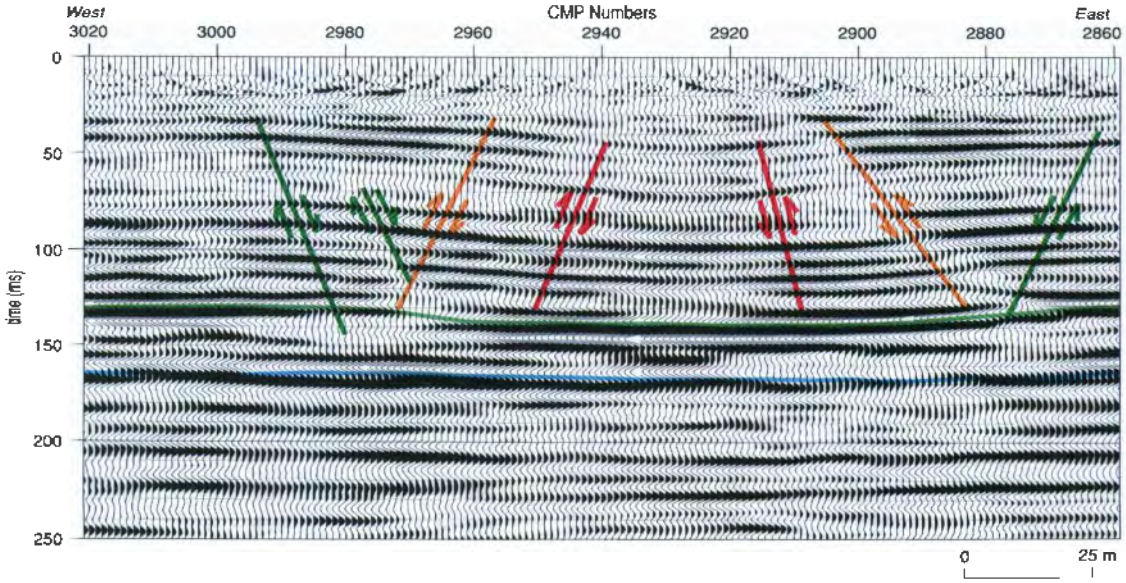

Figure 5. Paleosubsidence feature with no current surface expression. Dissolution of the upper portion of the salt is evident, with a high-amplitude reflection interpreted to be the top of salt. Failure likely occurred from middle of the feature out with the two pairs of reverse faults defining initial failure that occurred while the dissolution process was active, with normal-oriented offset beds in response to compaction into the dissolved and disturbed volume.

synform, the slopes are gentle and characterized by a block defined by normal faults. This asymmetry leads to the suggestion that the west side formed during initial subsidence and then overburden displacement halted, whereas the east side continued after initial subsidence to experience extensional stress and associated strain over a much longer time period.

Current sinkhole development at this site is related to the reactivation of natural leaching activities that originally produced the seismically imaged, 530-m-wide subsidence superstructure interpreted to have been active during the Tertiary and/or Quaternary. Alternately, recent surface subsidence could have resulted from localized failure of upper Permian rock layers previously bridging voids or settling of an undercompacted zone that formed while this paleosubsidence event was last active between the Tertiary and Quaternary.

Multiple episodes of natural dissolution and resulting subsidence can be localized, as in the previous two cases, or very expansive extending substantial distances along the regional natural dissolution front. Seismic investigation of a sinkhole located along the natural-dissolution front and coincident with an active oil field uncovered an extensive history of dissolution and associated subsidence (Table 1 ③). A portion of these seismic data almost 1 km west of the target sinkbole captured an extensive area of natural leaching that left a Permian rock sequence between the salt and bedrock surface that, while very irregular and distorted, retained sufficient trace-to-trace coherency to correlate reflections across the profile (Figure 6). Several chimney-collapse structures appear superimposed on a subsidence terrain characterized by short-wavelength undulations in overburden indicative of karst. These uniquely contrasting features and formation processes were clearly active at different times, but no signs are evident to suggest any current activity. In general, the ground surface in this area is topographically featureless and consistent with a broad alluvial-valley depositional environment.

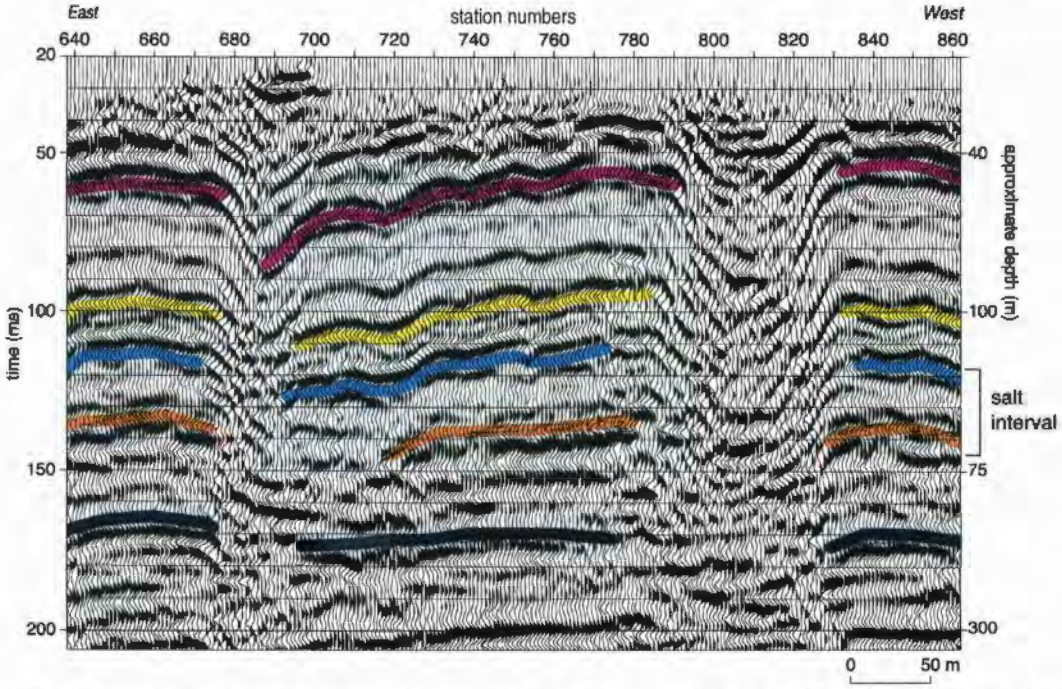

Figure 6. Complex paleosubsidence events spanning a distance of about 300 m located near the town of Punkin Center, Kansas. Undulating Upper Permian reflectors are representative of a very gradual subsidence process involving repetitive cycles of dissolution and subsidence.

These distinctive and abrupt paleosinkholes are within the Upper Permian portion of the section (above the salt interval). Subsidence geometries of these chimney-type failure structures appear to narrow very subtly in diameter between the salt and ground surface. Chimney-style features of this kind are routinely observed above salt-dissolution mines and borehole-induced dissolution failures where collapse was either rapid or dissolution hydrology was limited to a point source/exit. This seismic section captured the only known example of a highly disturbed and predominantly vertical failure feature that can be undeniably classified as a paleosubsidence event. Also of significance on this CMP stacked seismic section is the short wavelength, laterally undulating reflections and dipping beds that appear representative of a completely different dissolution and/or failure mechanism relative to the distinctive steep-sided chimney structures (centered on CMPs 690 and 810). For both the chimney and undulating drape-style failure features, no surface expression exists and the shallowest interpreted reflection events (Pliocene-Pleistocene Equus beds) appear flat with no expression of these underlying subsidence features, a situation indicative of subsidence dormancy since near the beginning of the Quaternary.

Clearly the overwhelming difference between this site and most others west of the dissolution front is the lateral extent of the highly distorted, short-wavelength undulation in the salt overburden. The presence of both styles of subsidence is suggestive of a changing hydrology, change in dominant leaching direction (vertical to form chimney and horizontal to form undulating reflections), and/or presence of zones within the salt susceptible to rapid vertical dissolution. Considering fluid densities and availability of fresher waters, it is reasonable to suggest natural leaching is predominantly active near the top of the salt. Normally interbedded shale and anhydrite layers act as permeability barriers where they tend to channel fluids more horizontally within the salt. These very vertical chimney features likely correlate to more solution-susceptible zones that have allowed enhanced fluid access and vertical movement in the otherwise locally continuous interbedded shale and anhydrite layers. No strong evidence exists on the seismic data to suggest tectonic forces have played a role here.

These steep-sided solution zones beneath stations 810 and 680 appear consistent with areas of depleted or nearly depleted salt volumes. Leaching likely originated at these locations along fractures prior to the predominantly horizontal dissolution that resulted in the more laterally consistent low-amplitude, short-wavelength undulations in the overburden. The horizontal leaching as evident from overburden subsidence has all the characteristics of a gradual process. Areas of greater solutioning are likely coincident with the troughs in the overburden reflection. Dissolution likely began at 810 prior to starting at 680, as evidenced by the overall gradual overburden-bed dip from west to east.

Based on reflection geometries, an alternate chronology is possible to explain these dramatic bed geometries. Reflections in very close proximity to the chimney features appear to correlate reasonably well across the chimney features. This observation could suggest the chimney-collapse structures occurred after or during the slower more laterally uniform dissolution and subsidence process. Alternatively, these short-wavelength bed undulations could be the result of different processes: dissolution, glide creep, and subsidence after the chimney features formed. This natural setting could provide the fluid and overburden pressure differential necessary to support either mechanism.

Multiple episodes of natural dissolution and subsidence evident on the Punkin Center (Figure 6) and the Victory Road seismic profiles (Figure 3) can be separated into different subsidence episodes based on unique characteristics and geometries, and therefore it is

reasonable to speculate as to rates and affected volumes associated with each subsidence event. Seismic-reflection sections from the Rayl sinkhole appear to tell a tale of an area influenced by several episodes of paleodissolution, each characterized hy distinct and seemingly disconnected subsidence locations as imaged throughout the overburden as distorted beds. These Rayl sinkhole data are suggestive of a very complex hydrologic past with multiple collapse features appearing to be the result of unrelated leaching activity spanning a generally large feature.

The Rayl sinkhole formed within several kilometers of the subcrop of the natural salt-dissolution front, gradually and inoffensively growing until it began affecting a county road, house, and an abandoned oil-field disposal well (Table 1 ④). Post-subsidence well integrity tests showed the casing of the disposal well was intact with no evidence to suggest it had lost containment or was responsible for this subsidence event. Seismic data clearly captured remnants of a complex subsidence history (Figure 7).

Surface subsidence tracked with ground-elevation surveys correlates the surface expression and its growth with the eastern edge of a paleodissolution feature captured on seismic data. The seismically imaged salt interval appears disturbed further east than evident in distorted reflections from the overhurden layers or ground surveys. Time delays and elevated reflection amplitudes from the top of salt along the eastern edge of this feature are consistent with the seismic characteristics of active dissolution in the salt. Rocks directly above the eastern dissolution front and immediately outside the volume defined by the reverse-fault planes (tensional dome) are likely under stress due to the apparent bridging of rock layers immediately above the salt interval. A large portion of the overburden rock imaged by the seismic section appears perched upon unsupported or poorly supported rock layers forming what geometrically

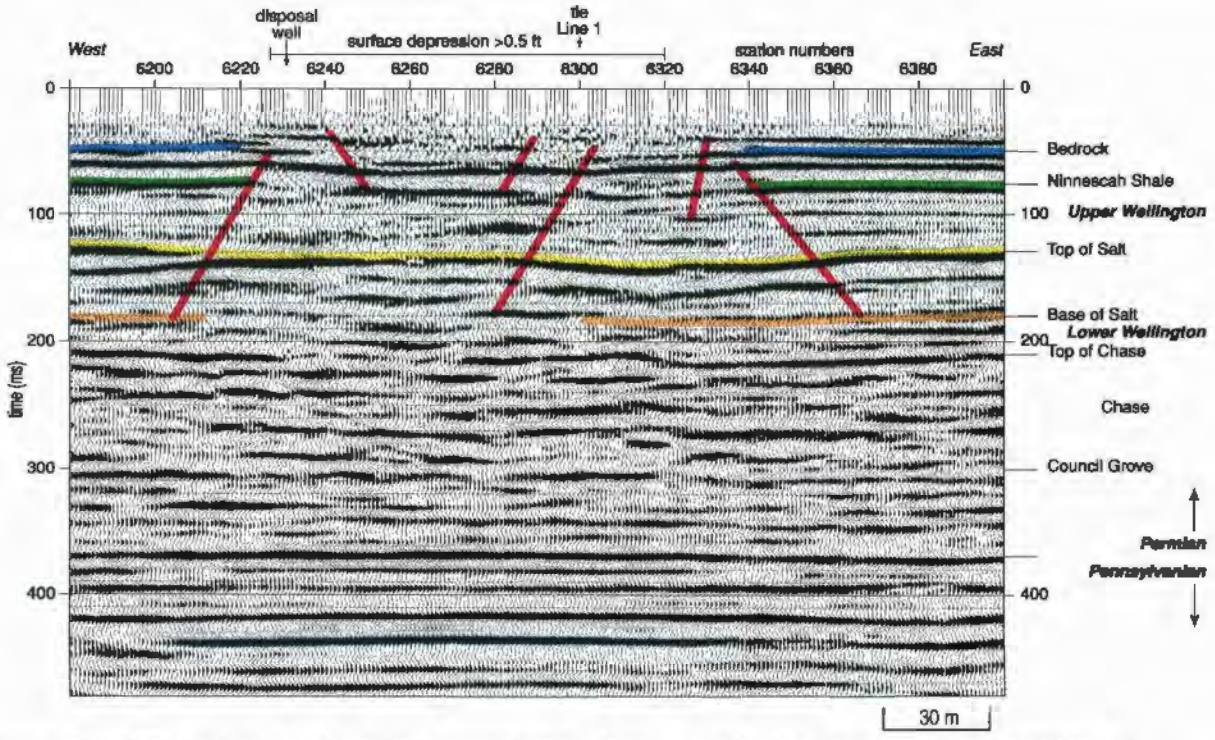

Figure 7. CMP stacked section with interpretation of reactivated subsidence feature beneath and immediately west of a house and major north/south county road. Current subsidence along eastern edge of dissolution zone is defined by reverse faults and is likely indicative of active leaching of salt beneath this section of line.

resembles a hanging wall. Stress within this hangwall will eventually manifest itself as strain after failure and formation of a normal-fault-defined bowl-shaped subsurface structure.

Disturbed layers between the top of the salt and the ground surface and the undulating reflecting surfaces within the salt itself on the west half of the seismic image are indicative of past dissolution and subsidence or creep events. Based on the subsurface history as interpreted from the seismic data, this area has undergone several episodes of natural dissolution of the salt and subsequent overburden subsidence. This extensive and complex subsidence history is not visible at the ground surface and therefore likely occurred prior to deposition of existing Quaternary surface cover. The well bore is located in the extreme western part of the affected subsurface and appears to be unrelated to current subsidence.

As will be shown later in this chapter, most dissolution sinkholes resulting from casing failure occur as a single, continuous dissolution and subsidence event that is centered on the failed casing. Based on the competency of the overburden and seismic-wavelet characteristics (velocity delays and elevated amplitudes at contact between dissolved salt volume and caprock or interbedded rock layers), dissolution responsible for the current sinkhole at the Rayl site is or was last active within a relatively small area along the eastern edge of what appears to be a large reactivated paleosubsidence feature.

Subsidence histories of active dissolution volumes are difficult to decipher when most or all of the salt have been leached away during multiple reactivations and hydrologic changes. As evident from the sequence of subsidence features presented so far in this chapter, with continued reactivation and depletion of salt stock, seismically imaged subsidence structures begin to lose their individual character and blend into a mass of distorted layers with only the personality of the whole remaining. A gradually subsiding sinkhole located near the natural-dissolution front began affecting a house and barn and was accused of being the offspring of dissolution induced by an early twentieth-century seismic-exploration shot hole (Table 1 ⑤). Shot holes of this type and era and in this area were deep (into the 50-m-deep salt) to optimize frequency and energy. They were rarely plugged, thereby providing a conduit for freshwater from near-surface aquifers to access the salt.

With the exception of a drop in signal-to-noise ratio near the middle of the section (location of the sinkhole), reflections from the upper 150 ms are coherent with geometries consistent with subsidence and bed distortion as observed at other sinkholes in close proximity and on the east side (minimal salt side) of the natural-dissolution front (Figure 8). Reflections from above the salt have geometries indicative of a relatively uniform subsidence history with predominantly brittle deformation. The general appearance and geometries of reflections above the salt are consistent with those observed on seismic data from the Punkin Center area (Figure 6) and Victory Road (Figure 4), more than 100 km north and equally close to the dissolution front.

These data have been flattened on the subsalt, Chase Group limestone to compensate for the extreme lateral variability in near-surface velocities that result from the irregular dissolution of the salt and associated overburden collapse. Based on the time difference between the Chase at about 130 ms and reflections within the Ninnescah Shale, located immediately above the Hutchinson Salt Member, some salt still remains at this site. There appears to be as much as 10 ms more salt at the west end of the profile relative to the east end. From the very erratic nature of the reflections above salt, small-scale (50-m radius) dissolution of the salt varied noticeably across this site. Reflection geometries are suggestive of overburden collapse influenced by meandering fluid pathways altered as each subsequent roof section collapsed into

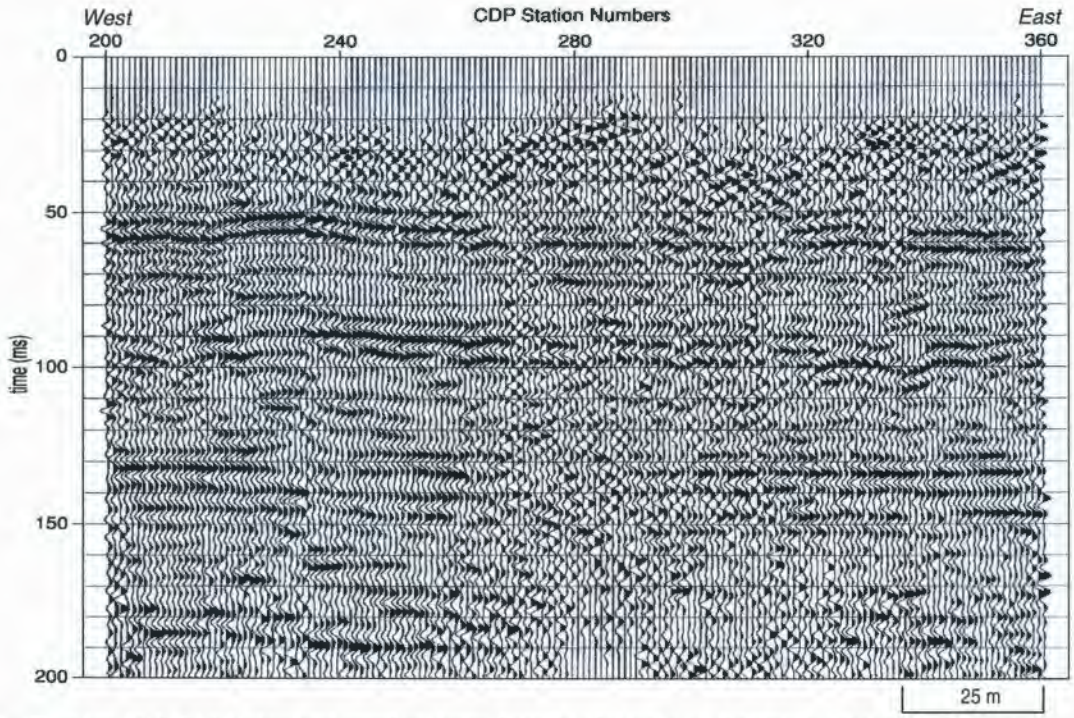

Figure 8. Twelve-fold CMP stacked section from Buerki sinkhole in Sedgwick County, Kansas. Reflection from base of salt flattened to compensate for near-surface velocity irregularities. Reflection undulations consistent with those seen on Figure 6 where natural dissolution resulted in similar gradual subsidence features.

leached voids. Plastic-looking deformation is consistent with horizontally elongated leach zones large enough to instigate roof failure followed by upward migration of the void through each layer with successive roof failure. Individual vertical collapse distances are likely quite small, resulting in very localized fractures and fault zones with offsets below the horizontal resolution of these data and therefore the plastic appearance of the bed deformation.

Natural-dissolution features on the basinward (toward the thicker salt interval) side of the regional dissolution front are much better preserved than those on the east, allowing more confident event chronologies to be interpreted from seismic-reflection data. In areas near the dissolution front and on the west side, like the Punkin Center site and Victory Road sinkhole, the salt is still relatively thick, with dissolution and subsidence still in the early stages. In an area 20 km north of the Punkin Center and Victory Road seismic profiles, the dissolution front is defined by an extremely high salt-isopach gradient transitioning from full salt thickness (125 m) to less than 10 m in less than 1 km, based on well data.

A site where this high-gradient dissolution front is mapped to cross the planned construction of a new superhighway prompted a high-resolution seismic-reflection study (Table 1 ⑥). Special emphasis was placed on locations where rigid structures (bridges and overpasses) were planned. Of primary concern were locations with the potential for catastrophic surface collapse as inferred from voids and disturbances interpreted on seismic sections from the salt, anomalous reflection characteristics in the shallow portion of the section, or areas where seismic-reflection wavelet properties are consistent with active dissolution. However, in general, the objective was detection of any subsurface feature that could threaten highway stability and public safety. Considering the relative proximity of this Inman profile to the regional dissolution

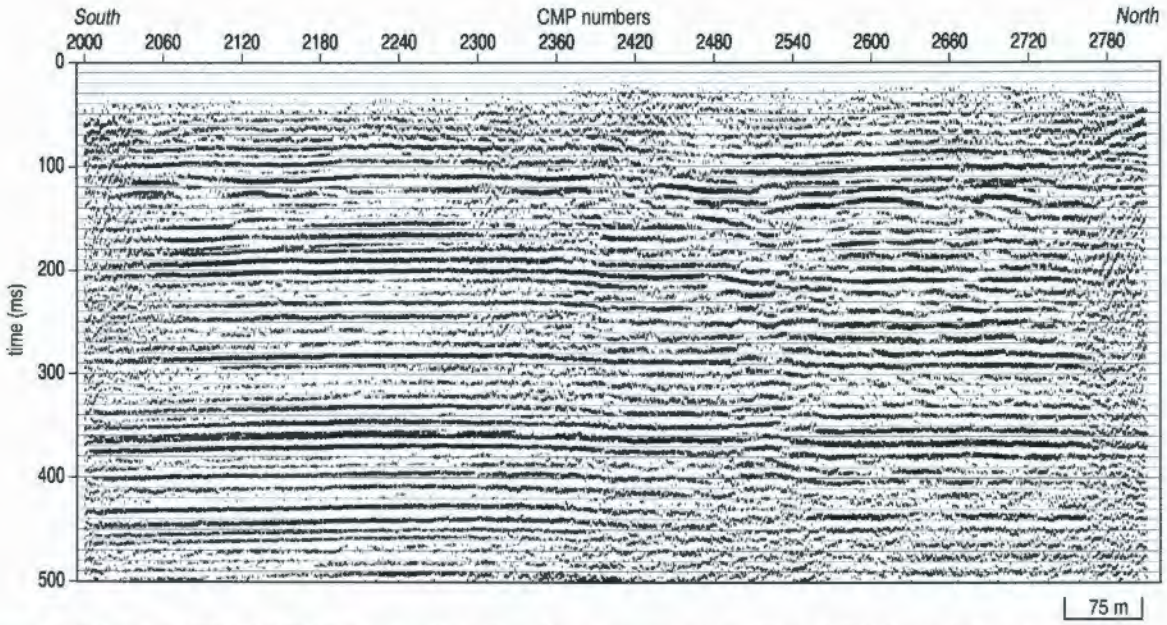

Figure 9. Nominal 60-fold CMP stacked section from Inman area. The drill-inferred dissolution front along the eastern edge of the Hutchinson Salt Member is evident based on appearance of highly distorted reflection with obvious static associated with a laterally variable velocity profile.

front, characteristics of seismically imaged dissolution structures were expected to be similar to those observed on two previous studies at Punkin Center and Victory Road. The 10-km-long survey was designed for optimal subsurface imaging oblique to the high-gradient contours of the salt isopach.

Consistent with the zone projected by well data to possess the most rapid thinning of the salt layer, seismic data imaged a highly altered near-surface geology (Figure 9). An abrupt change in reflection characteristics at CMP 2300 likely marks the western edge of the rapidly thinning salt interval defined as the natural-dissolution front. The transition is obvious and characterized by relatively well behaved reflections to the south changing to highly altered reflection events within the 70-m-thick salt over a distance of less than 100 m. As expected, the salt topography changes very abruptly, with undulations in reflections (nodes) as high as 100 m over distances as short as 250 m. This very ragged nature of the dissolution front has been suggested but never imaged (Spinazola et al., 1985).

Reflections interpreted within the Permian shales and above the dissolution-altered inter-salt reflection events appear indicative of only minor overburden subsidence immediately above the leached salt section at this location. Reflection events above the altered salt possess minimal drape or deformation in response to what seismically resembles significant dissolution and deformation within the salt interval. The reflection immediately above the salt at approximately 80 ms possesses a maximum of 10 ms of time change across a broad synclinal structure approximately 700 m in length. This 10-ms drape on the 80-ms overburden reflection is likely in response to the over 20 ms of subsidence and bed aberrations evident within the salt interval over a distance of around 400 m. As well, the 80-ms reflection possesses a very smooth synclinal geometry consistent with relatively small-scale brittle deformation along subresolution fault and/or fracture zones. Contrast this smooth 80-ms overburden reflection with salt reflections immediately below that appear irregular—steeply dipping in some places—and that possess

unequivocal brittle deformation characteristics indicative of a transition from high energy within the salt interval to a low-energy environment in the predominantly shale overburden. Deformation above the salt has a plastic appearance when, in reality, distortion of these beds has occurred through brittle deformation; however, as previously stated, data resolution is not sufficient to detect small-scale faults and fractures.

Based on the appearance and severity of the dissolution-altered salt reflections between 100 ms and 150 ms, more short-wavelength synclinal-shaped subsidence features were expected than observed in the upper 80 ms of overburden along the interpreted dissolution edge north of CMP 2360. These expected short-wavelength subsidence geometries were observed on the Punkin Center line, Victory Road line, and Buerki line. It appears initially at the very edge of the highly active dissolution front that shale layers in the overburden tend to distribute deformation over a larger distance, resulting in a more plastic-appearing subsidence in spite of the fact microscale faults and fractures are responsible for these structures. Deformation in the salt layer is more isolated and rugged interpreted around void areas where leaching appears to have been more aggressive with deformation focused within the salt. Clearly this plastic-appearing deformation in the overburden is a symptom of the minimal strength these shales possess as roof rock and a high density of small-scale fractures and faults.

Layers within the solution-disturbed salt appear to have failed in a brittle fashion, forming a series of highly distorted reflections that lack geometric consistency and possess notable diffraction events. These bed-termination characteristics suggest the permeability barrier these interbed layers once represented are likely breached at various locations across the dissolution front and have allowed fluids greater freedom to move through the salt. This suggestion is consistent with the two different dissolution and associated deformation mechanisms observed beneath the Punkin Center profile with the more horizontal, gradual subsidence preceding the more rapid, vertically elongated compressional-style chimney failure.

Estimating the amount of subsidence would best be accomplished using an accurate time-to-depth converted seismic section; however, due to the extreme distortion in reflecting events, CMP stacking velocities calculated from these data lack the necessary accuracy. Two different velocity aberrations present problems for developing depth-based geologic models in subsidence areas. First, the dissolution zone itself has significant void space and rubble in areas where surrounding rock is competent and consolidated. This results in a lower average or bulk velocity, which manifests itself as reflection pull-downs on CMP stacked sections below the dissolution zone. Reflections from below the dissolution zone appear to possess subdued structures (deeper time-depth than the dissolution zone) that mimic those from above the dissolution zone. If an accurate, subspread-length velocity function could be determined, the seismic two-way traveltime section could be converted to a depth section with accurate geological and structural interpretations of the rock layers in the subdissolution zone. This has been problematic for many petroleum-exploration seismic surveys where evaporites are present above the reservoir.

A second velocity abnormality unique to and complicating interpretations of subsidence features on time sections is reduced average velocity above the dissolution zone due to settling and degradation of the rock matrix from fracturing, distortion, and differential compaction. Unlike the shadow effect that dissolution and related subsidence have on deeper events, this velocity effect is related to true rock properties and geometries within the affected portion of the seismic section. A consequence of these inaccurate velocities is unrealistic time-to-depth conversions. In spite of structurally misleading seismic-depth sections, the general geometry of these physically altered layers as depicted on CMP stacked time sections do reasonably represent

the subsurface. Interpretations of events above the dissolution zone from time sections alone are reasonably consistent with the true geology (although slightly exaggerated).

Immediately south of the edge of the dissolution front (~CMP 2300) is a relatively small (~150 m wide), yet distinct seismic feature centered on CMP 2150 (labeled A on Figure 10). This reflection, interpreted to be from or at least near the top of the salt, has wavelet characteristics consistent with expectation based on models and previous seismic studies for the dissolution-altered top of salt. Most notable is the very subtle yet vertically isolated synclinal shape of the single reflection from the top of the salt (~110 ms) (labeled A on Figure 10). Maximum time displacement of the salt reflection at the center of this bowl (synform) feature is around 5 ms. This subtle drape in the top of the salt reflection is consistent with other seismic observations associated with leaching near the natural-dissolution front.

This feature provides the first opportunity to correlate seismic-wavelet characteristics and reflection geometries to dissolution, using proximity and models as guides. Consistent with theory, amplitude is the attribute keenly sensitive to voids and/or altered zones beneath continuous spans of roof rock or interbedded layers. Comparison of the salt-reflection wavelet amplitude from within the interpreted subsidence feature centered on CMP 2150 with the same reflection from what geometrically and from velocity analysis appears to be an undisturbed section of salt centered on CMP 2240 (labeled B on Figure 10) highlights a marked increase in amplitude inside the bowl-shaped subsidence feature. This same phenomenon was noted on reflections from U.S. 50 (Figure 2), Victory Road (Figure 3), and Rayl (Figure 7).

Some evidence exists on these data that frequency might also be affected by changes due to minimal localized leaching. This frequency characteristic would be expected in reflections from the shadow zone below void areas. The rubble zone should both scatter and attenuate greatly the high-frequency portion of the spectrum relative to equivalent energy traveling through competent rock immediately adjacent to the subsidence-altered rock. Some of the most compelling evidence supporting many of the concepts developed in this manuscript describing

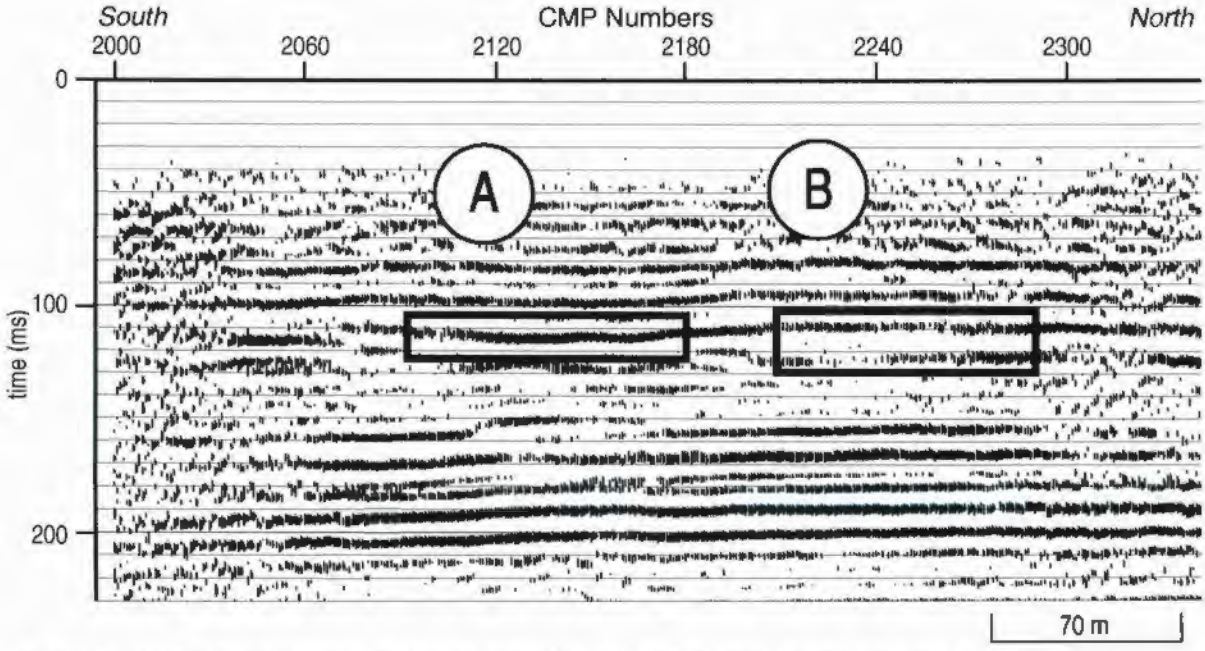

Figure 10. (A) Solution-altered reflection wavelet; (B) native from Inman seismic profile.

the natural dissolution process has been based on reflection-amplitude anomalies associated with dissolution at the salt/shale caprock interface.

Seismic Investigations of Anthropogenic-dissolution Subsidence

Hydrology is the component of dissolution-instigated subsidence that most significantly distinguishes anthropogenic from natural processes. With the fluid-access points (inlet and exit) fixed for the anthropogenic-induced dissolution case, the process is clearly constrained to a volume of salt commensurate with the dynamics of the fluid and available salt stock. Although in general the processes are identical, resulting structures, fluid volumes/velocities, and time frames are dramatically different. Consistent with the previous section, where discussions focused on seismic investigations of natural subsidence features, the remainder of this chapter will highlight seismic investigations and associated findings at anthropogenic-dissolution sites, starting with simple single-stage collapse structures and working toward complex subsidence structures with multiple collapse episodes and changing stress regimes.

A gradually subsiding sinkhole centered on a saltwater-disposal well formed between a major highway, a set of railroad tracks, and a farmstead and posed a potential risk to public safety (Table 1 ⑦). A set of seismic-reflection profiles acquired directly over the sinkhole was used to identify the sinkhole's subsurface expression (Figure 11). This sinkhole and associated subsurface feature is symmetric about the failed borehole and clearly possesses two different subsidence geometries. Based on this and previous sinkholes studied, initial failure was confined between reverse-fault planes inferred to be consistent with the lines of stress in the overburden above a void volume just prior to initial roof-rock failure and associated overburden collapse. Once this initial failure occurred, collapse of rock layers within the overburden continued along

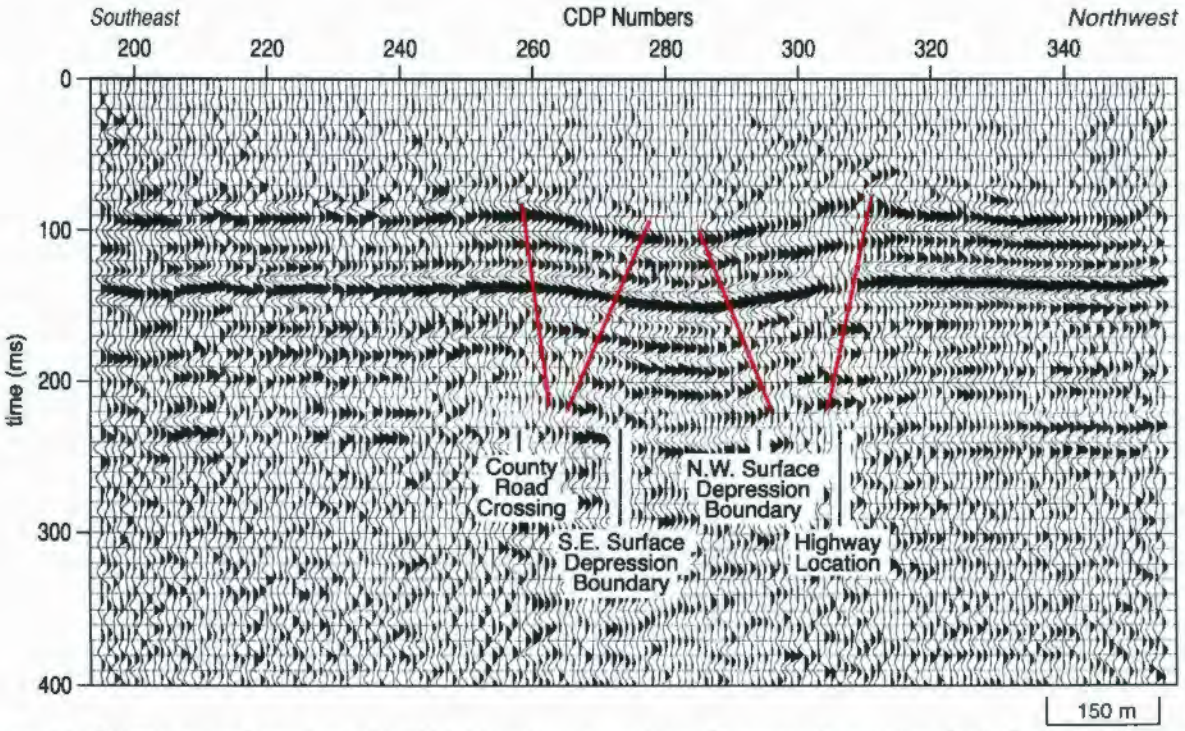

Figure 11. CMP stacked section with 12-fold redundancy from Conoco disposal-well sinkhole in Ellsworth County, Kansas. Symmetric subsidence structure and excellent reflection coherency from rock layers above the salt interval at about 240-ms two-way traveltime.

more normal fault planes defined by bed offsets. This extensional-failure mode (secondary) is consistent with the change in stress field after initial collapse, assuming the salt void did not experience continued dissolution growth.

This interpreted sinkhole chronology clearly fits the empirically derived model where initial roof-rock failure is controlled by the stress field and strength of roof rocks. Subsequent failure/relaxation of overburden appears consistent with an extensional setting where compaction, rock strength, and overburden load dictates bed failure, geometries, and subsidence rates. Using the current working theory suggesting that once secondary subsidence begins to occur (bed offsets mapped with normal-fault geometries) and void growth slows or halts, this sinkhole's horizontal growth should be slowing and subsidence rates decreasing. Seismic images of the post-failure subsurface at this sinkhole are consistent with a single episode of dissolution and then failure, beginning with compressional and ending with tensional.

Induced dissolution (anthropogenic) is generally characterized by a relatively localized disturbed volume and symmetry about the borehole. As in the previously documented sinkhole and associated seismic image, the growth rate of surface subsidence is generally relatively uniform. A subsidence event clearly related to a failed disposal well displaying asymmetric rates of subsidence, and with the culprit well significantly offset from the center of the sinkhole, provides more empirical details of these stealthy hazards (Table 1 ®). Observations related to a lack of symmetry were of sufficient concern to prompt authorities to investigate the subsurface with a low-fold 3-D seismic-reflection study and five 2-D profiles encompassing the surface depression. Results from this seismic study were intended to establish some degree of confidence in the safety of crews commissioned to reoccupy the borehole and plug the casing below the salt interval.

From the CMP stacked section the subsidence chronology and current potential for rapid failure within the collapse feature can be diagrammed (Figure 12). Based on previous studies of subsidence induced from salt-dissolution mining and seismic images acquired at the very early or active dissolution stages, it is reasonable to interpret two different collapse periods/mechanisms. First, the salt void grew beneath an impermeable, insoluble layer of shale or anhydrite (could have been at the top of the salt or one of the interbedded layers) until the unsupported span of roof rock exceeded the strength of the roof rock and failed consistent with the tensional dome. Vertical migration of the void proceeded through each successive layer of rock, moving ever closer to the ground surface. Collectively these successive bed ruptures manifested themselves in an upward-narrowing chimney-type geometry consistent with reverse faulting. As noted in previous chapters, this phenomenon has been detected by borehole interrogations at sites where sinkholes had formed from catastrophic collapse of salt jugs.

Seismically imaged rock layers around the perimeter of the collapse structure show evidence of bed-offset geometries consistent with normal faulting. Normal faults, interpreted on these seismic sections outside the central reverse faults, are indicative of a complete reversal of stress marking the termination of the compressional stress and buildup of extensional stress. This change is completely consistent with the concept of an extensional stress environment being established once there is no longer horizontal growth via dissolution of the salt interval. Surface subsidence at this site slowed to less than 1 cm/year from over 20 cm/yr over a 10-year period starting with the initial formation of the depression.

Borehole-induced dissolution and resulting subsidence as described by the previous two examples was clearly a single-episode event with initial upward migration of the dissolution void defined by compressional-stress-induced roof stoping and bed collapse followed by what appears

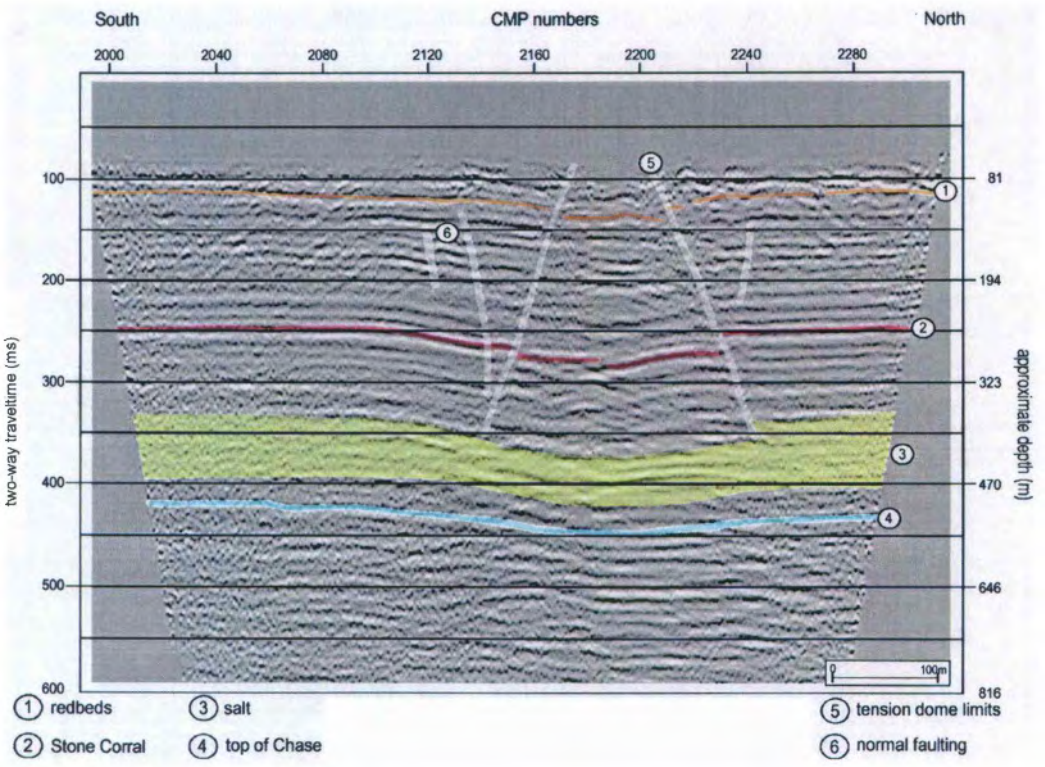

Figure 12. Nominal 48-fold CMP stack of reflection data acquired around and through the French sinkhole. Strain geometries are very evident with reverse faults defining subsidence near the center of the feature and normal relative bed movement in the outer part of the subsidence features.

was a uniform transition to extensional-stress-controlled failure and lateral expansion. For both anthropogenic- and natural-dissolution-induced subsidence, seismic images appear to consistently provide evidence supporting both compressional- and extensional-failure modes. The one key characteristic that distinguishes these two hydrologic classifications is the episodal nature of natural versus the somewhat continuous progression through the stages for anthropogenic-induced subsidence. To continue improving the working model, seismic images of a subsidence event with an active sinkhole currently undergoing salt dissolution and therefore possessing a complex stress regime will be considered. This next setting tests the theory that movement along both reverse and normal faults can be active simultaneously when leaching along the dissolution-void perimeter is active.

Seismic-reflection imaging provided an enlightened view of the subsurface beneath two distinct, circular, and gradually subsiding sinkholes first discovered in 1966 in the Gorham oil field beneath a stretch of four-lane highway (I-70) crossing north-central Kansas (Table 1 ⑨). Considering the average square kilometer in this oil field has more than 50 documented well locations, subsidence associated with abandoned oil or disposal wells should not be unexpected and could occur almost anywhere, at any time, along this several-kilometer stretch of highway. Around 10 cm per year of subsidence has been measured at the primary sinkhole (Crawford) since discovery. Seismic data acquired in 1980 and again in 2005 provided important information concerning sinkhole development and potential future growth projections.

The seismic expressions of the two principal sinkholes are as obvious on the CMP stacked section as they are on the ground surface (Figure 13). A unique characteristic of these

two sinkholes, at least compared to the two previously discussed borehole-induced dissolution and subsidence features, is the very vertical nature of the bed offsets. Images of reflectors below both these active sinkholes appear to possess the same chimney-style, vertical-collapse structures observed and interpreted on seismic data over salt jugs after roof failure, and consistent with initial failure along the lines of equal stress, to define the tensional dome.

Based on drilling completed during the late 1990s, the ruptured casing at both these sites is actively moving fluids out of the salt interval. Bed-offset geometries observed on the CMP stacked sections associated with these sinkholes are consistent with previous interpretations of initial failure on seismic data from other borehole-induced dissolution and collapse structures. From interpretations of paleosubsidence features captured on seismic sections near the natural-dissolution front (e.g., Figure 4), episodic reverse-fault-controlled subsidence appears to be coincident with unique periods of reactivated leaching with associated stress release. It is, therefore, reasonable to assume that subsurface subsidence structures with steep-sided, chimney-type structures (consistent with the tensional dome model) are indicative of either active or very recently active dissolution. Neither of these subsidence features possesses reflections with significant bed offsets displaying normal-fault orientations. It is, however, plausible to suggest that a few bed offsets can be interpreted with normal-fault orientations in the upper 200 ms and within about 50 m of the extrapolated intersection of the ground surface and reverse-fault planes. Extending that interpretation one step further, it is reasonable to suggest dissolution has halted when subsidence can clearly be defined by normal-fault planes that extend from the salt to the ground surface on seismic-reflection images.

A small sinkhole centered at approximately CMP 1700 appears uniquely different relative to either of the seismically imaged larger active sinkholes (Figure 13). Beneath both the two large active sinkholes, the high-amplitude reflection event at approximate 260 ms (Stone Corral Formation) has either failed or has been distorted beyond what these data can resolve. As well, an abundance of diffraction events can be interpreted from around the perimeter of the large subsidence features, indicative of bed terminations. Also the interpreted offset geometry of reflectors within these two sinkholes is consistent with the previously described reverse-fault

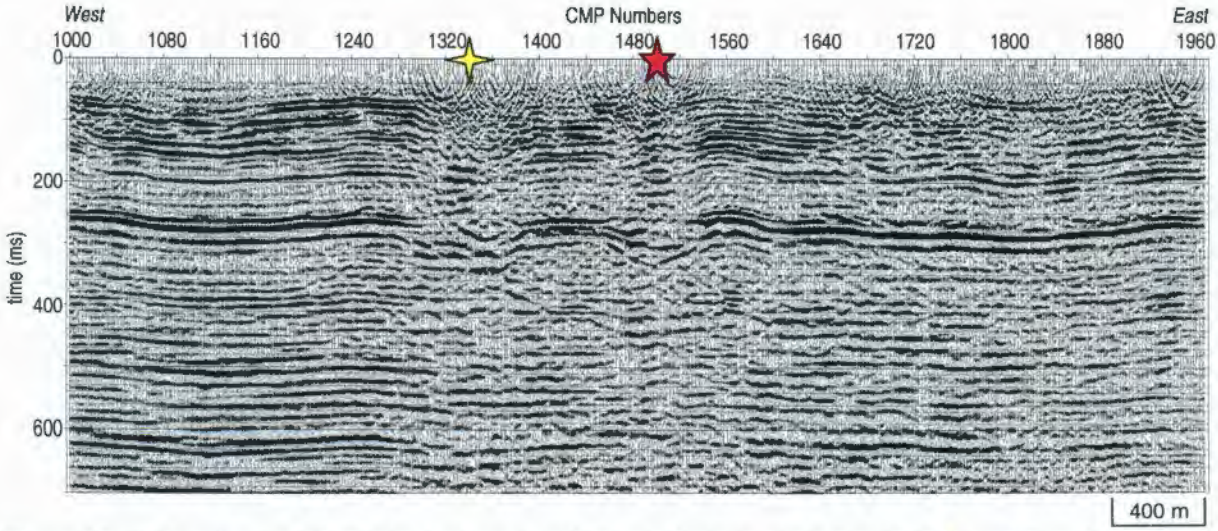

Figure 13. I-70, migrated CMP stacked section: Witt sinkhole is at station 1340✧ and Crawford is at 1500★. The high-amplitude event at 260 ms is the 300-m-deep Stone Corral Formation. Top of salt is at about 400 ms and approximately 400 m below ground surface. Static effects from lateral variability in velocity are evident on the Stone Corral as a result of both dissolution and near-surface deposition.

model. Subsidence features imaged on the eastern third of the 5-km-long seismic profile possess subtle drape with a general appearance more consistent with the single-episode borehole-induced subsidence feature introduced at the start of this section (Figure 11). It is, therefore, reasonable to suggest the subsidence and/or dissolution mechanism or process in this third subsidence area is somehow different from either of the two large active sinkholes to the west.

Closer study of this small sinkhole uncovers evidence of another subsidence feature centered on about station 1840 that has not yet made a depression at the ground surface. For both these smaller sinkholes, the Stone Corral Formation (immediately above the salt interval) possesses about 20 to 30 ms of drape or flexure. The fact that this layer has not ruptured sufficiently to distinguish bed offsets on seismic data suggests either dissolution has been predominantly horizontal in nature (much like that suggested for natural dissolution) or it has been very localized and has not yet produced an unsupported span of roof rock large enough to exceed the strength of the immediate overburden layers in the Cretaceous portion of the section. One more possibility is that the dissolution process here has been halted due to an interruption in fluid movement.

As previously discussed, with the dramatic drop in localized velocity within the disturbed rock volume during the upward migration of a dissolution void comes significant statics problems, and, without a highly detailed velocity function, time-depth conversions are extremely inaccurate. So to more accurately represent the time structures above these subsidence features, reflections between the base of the salt and basement were time-flattened. This process reduces any static effects and more accurately represents the time structure of the synclinal features evident on the 260-ms-deep Stone Corral Formation (Figure 14). Reflections above the 330-ms salt are obviously distorted across most of the eastern half of the profile while the reflection events below 400 ms are flat with no evidence of near-surface static.

Several distinctive episodes of subsidence can be inferred from the small, unique synclinal structures that appear to distort the Stone Corral Formation and overlying shales and sandstones in the Upper Permian and Lower Cretaceous. Considering the well density in this oil field, it is likely the subsidence features observed on seismic data on the eastern half of the line are the result of wells that have either leaked or with annular space that did not hydraulically isolate the salt from aquifers throughout the upper 1.5 km. Hence, dissolution of the salt was active for shorter periods of time, less fluid was available to enlarge voids sufficiently to

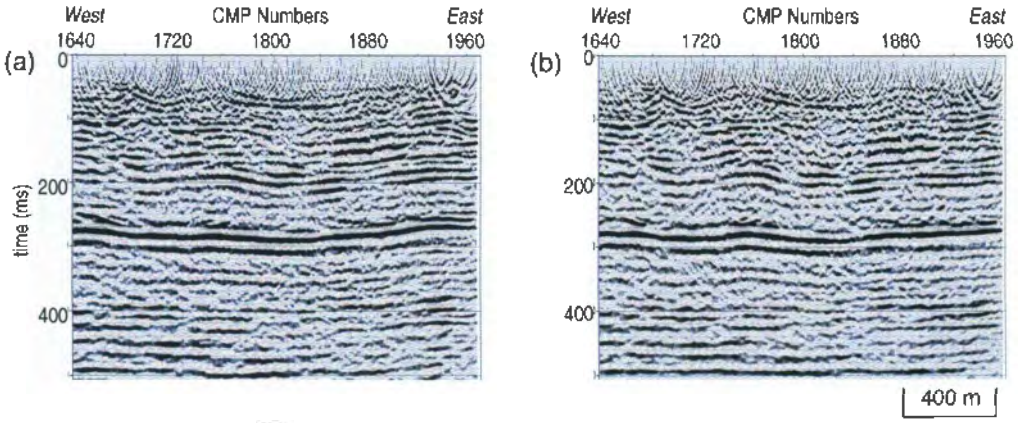

Figure 14. A portion of the CMP stacked section from Figure 13 (a) has been time-flattened on the subsalt reflections (b). Artificially flattening reflections immediately below the salt interval reduces the effect of velocity variability and focuses reflector structures above the base of the salt.

consume enough overburden to form a significant collapse structure, or leaching was predominantly in thin zones along the top of individual salt layers.

Subsidence artifacts imaged beneath the two active sinkholes that are interfering with the four-lane I-70 highway in north-central Kansas are distinctly different compared to the previous two anthropogenic cases where dissolution had halted and subsidence was occurring within an extensional environment. The I-70 sinkholes appear to be forming under the influence of active dissolution and therefore a compressional-stress environment seems to still be present. Consistent among these last three sinkhole studies is the symmetry of formation. In all the previous studies these seismic-reflection images of the subsidence structures have suggested a relatively uniform radial development. In the next study, time-lapse seismic images provided the first-ever glimpse of a borehole-induced subsidence feature that formed catastrophically and continued to develop along an elongated solution-controlled alley.

Formation of the Macksville sinkhole was catastrophic and anomalous; therefore, it has generated a lot of interest and speculation as to the formation mechanism and subsurface chronology (Table 1 ⑩). This sinkhole formed catastrophically around an abandoned oil-field brine-disposal well. Failure at this site came with no warning and in a portion of the oil field that had been shut-in for over two decades. Concern for ground water in this area and risk of ground movement beneath surface installations supporting active oil production prompted the seismic investigation of this sinkhole.

Due to the large pond (approx. 2500 m^2) in the center of the sinkhole, which was approximately centered on the disposal-well location, seismic lines were acquired off sinkhole center and for the west/east profile along a stretch of ground with little to no surface expression. The extremely steep-sided nature of this sinkhole on the south, west, and north restricted optimum placement of seismic lines. However, key subsurface characteristics of this actively growing sinkhole were interpreted in spite of the less-than-ideal line placement. Clearly this subsidence feature can be characterized by well-defined reverse faults defining the subsurface boundary of the initial failed rock layers (Figure 14). On this CMP stacked section, there is no clear indication that bed-offset planes are consistent with normal-fault geometries. Considering this sinkhole formed more than 10 years prior to the seismic survey, it is a bit surprising that the active/current failure mechanisms for this sinkhole are still characterized by bed offsets with reverse-fault orientations.

As expected, the shallowest layer imaged on the west-to-east line shows no indication of subsidence (Figure 15). This is consistent with the fact that this survey line was immediately south of the surface rupture in an area with no topographic expression of the sinkhole. Clearly the root of the sinkhole extends under the 2-D profile line and, based on the increasing diameter with depth of this feature, the subsidence geometry is still dominated by reverse faulting. Consistent with inferences from studies previously detailed in this section, this apparent compressionally dominated stress regime is likely indicative of active leaching and void building. Once dissolution stops and active void growth ends, the dominant-offset orientation of rock failure should be extensional.

Along the eastern end of the sinkhole the topography changes gradually enough to allow the north/south line to be acquired within the eastern rim of the sinkhole trough (Figure 16). The reverse-fault bed offsets defining the core of this subsidence feature are well imaged and easily interpreted. Unique about this profile relative to the west/east section (Figure 15) is the apparent normal faulting (CMP 4120) that can be interpreted immediately north of the upthrown side of the outermost reverse faults. By incorporating observations from previously studied sinkholes, it

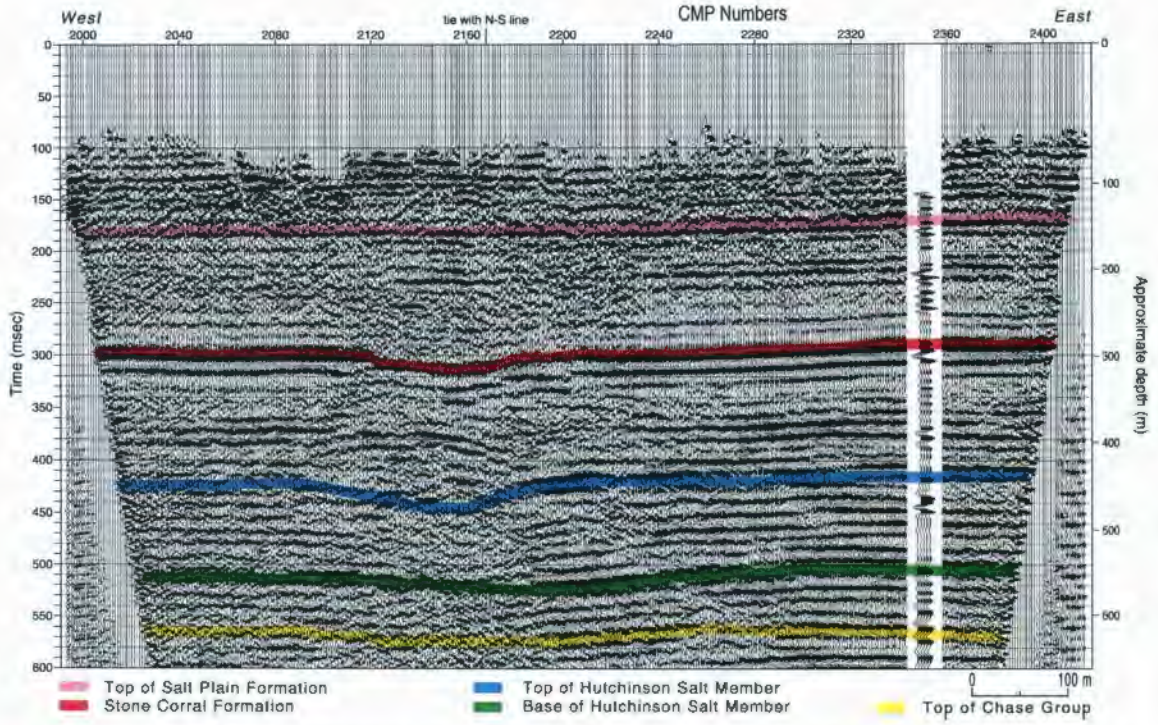

Figure 15. Nominal 60-fold interpreted CMP stacked section from the Macksville sinkhole. Shallow reflections are from rock layers yet unaffected by the subsidence feature while deeper rocks are clearly suggestive of a reverse-fault offset geometry in reflection from the top of salt to about 200 m.

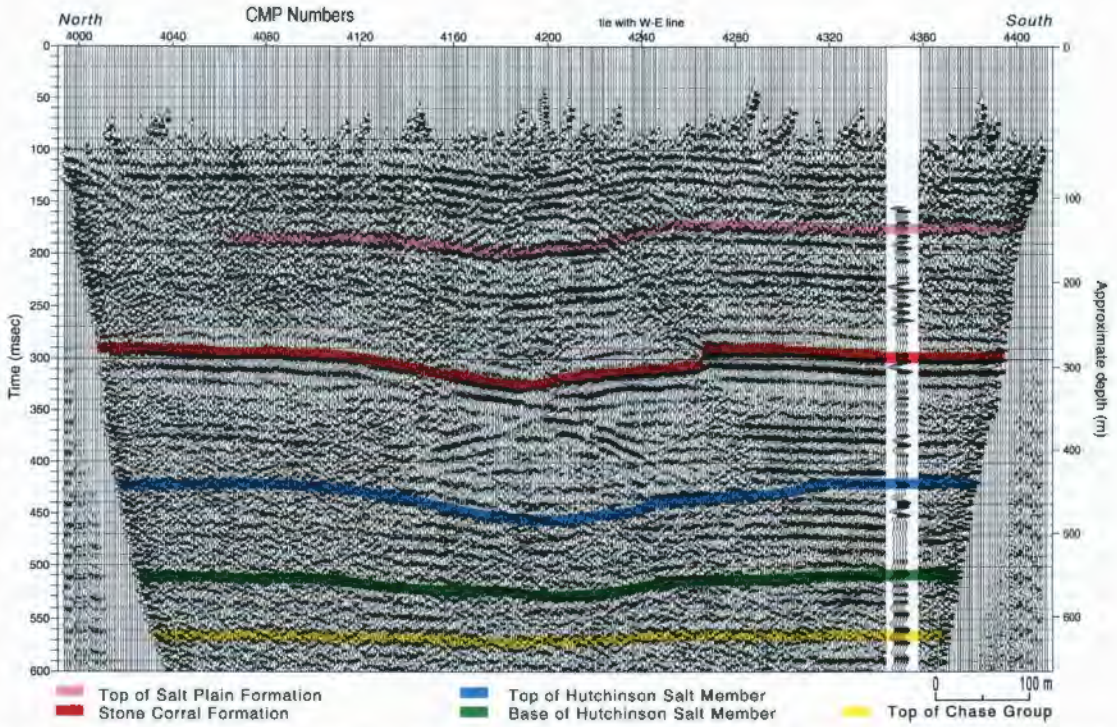

Figure 16. Nominal 60-fold interpreted CMP stack of north/south line at Macksville sinkhole. Drape in reflections is evident to the top of the section consistent with the location of this line, which crossed over the east edge of the sinkhole. Reverse-fault geometries dominate the interpreted bed offsets.

is reasonable to suggest that migration of the dissolution front to the north has ended, as indicated by the apparent change in the stress regime in that quadrant. Migration of the dissolution front appears active to the west, south, and east. This subsurface observation is in complete agreement with surface-elevation surveys that have been carried out each year since the sinkhole first formed.

Borehole-induced dissolution and resulting subsidence features provide ideal settings for studying the controlling processes and characteristics of leaching interpreted from reflector-defined collapse structures (in a few cases where time-lapse surveying has played a role; changes in those geometries). Seismic images of reflectors beneath a sinkhole are a compilation of interrelated clues that can be used to unravel the history of the process. By carrying forward lessons learned during study of progressively more complex cases, an evolutionary chain of events develops that can guide empirical models used for predicting future growth scenarios as well as giving insights into the past. In this section discussions started from the simple first-order continuous subsidence feature and have advanced to a complex subsidence feature defined by a non-uniform geometry and active salt harvesting well after catastrophic sinkhole formation. Emerging from a synthesis of the past four cases is a definable pattern and series of events that seem to collectively describe the many types of active processes. The next sinkhole and associated subsidence structure discussed adds a significant level of complication through the involvement of more than one well bore and communication between those wells.

A loss of well-bore confinement was observed during standard pressure tests, cluing regulators into a potential problem isolating well-bore fluids from surrounding evaporite layers at a disposal well in south-central Kansas (Table 1 ⑩). Attempts to plug the well and seal the borehole failed. With the casing severed, borehole fluids were moving easily through the salt, leaching of that salt was apparently uncontrolled, and a gradually subsiding and expanding sinkhole was developing. It was soon discovered that a second borehole less than 100 m from the first had also lost containment and the two were hydraulically connected. Based on well-bore tests the worst case was discovered—fluid was moving within the salt interval between the two wells.

Reflections in proximity to and beneath the sinkhole were highly distorted with a collapse structure well defined in the subsurface (Figure 17). Subsidence geometry of the 220-ms-deep Stone Corral Formation is unique compared to previously studied single-well sinkholes where salt was at a similar depth and dissolution was instigated by oil-field well-casing failure. At this site it appears the Stone Corral Formation failed as large, relatively intact blocks with the largest segment measuring around 150 m to 200 m in length and down-dropped around 40 m (after compensation for the reduced average velocity within the disturbed near-surface) located immediately beneath the sinkhole. Other large pieces of this anhydrite layer appear to have tilted in response to progressive leaching of the salt and expansion of the dissolution front.

Interpreted bed-offset geometry/orientation is unique to this subsidence feature and provides important clues to possible growth mechanisms. Faults interpreted as defining layer displacement resulting from failure are different on one side of the subsidence feature relative to the other. As with all other subsidence features studied in this chapter, opposing reverse faults clearly define the initial failure cone and are centered on the current sinkhole at about CMP 2360. Based on surface-elevation data, the most rapid vertical growth is along the eastern side of the sinkhole, while very little vertical growth has been observed to the west; the sinkhole clearly possesses a very gentle ground surface slope toward the sinkhole center from all directions.

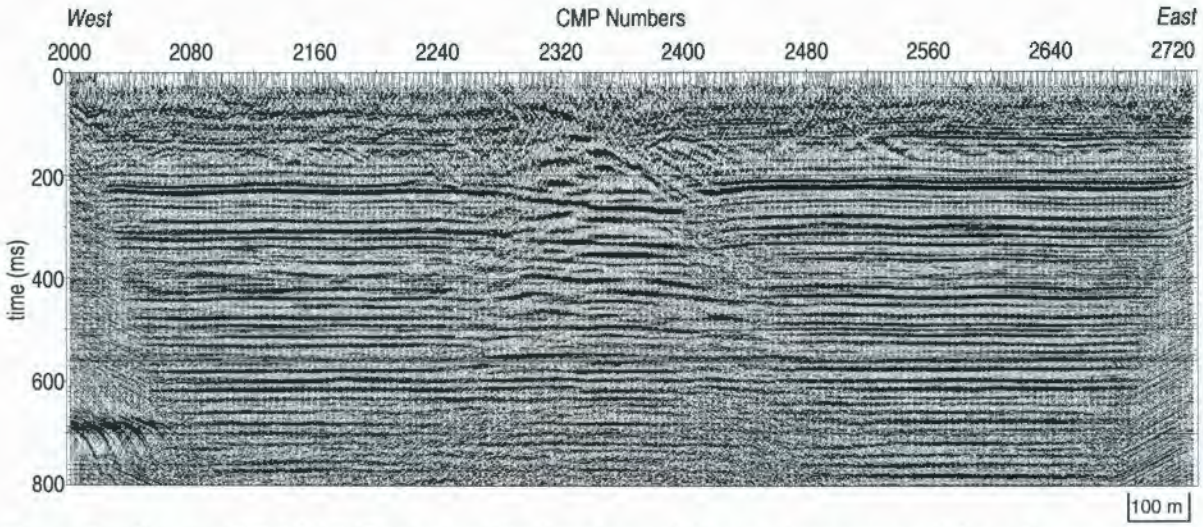

Figure 17. Nominal 60-fold CMP stack at the Leesburg sinkhole. Asymmetry of the collapse structure is unusual for a subsidence feature from borehole-induced dissolution. East side of profile is clearly defined by reverse-fault geometry.

It is reasonable to correlate future surface growth with the unique reflection geometries on opposing sides of this subsidence feature. Gradual expansion in the radius of the sinkhole to the west is consistent with normal-fault offset geometries in bedding as would be anticipated during gradual relaxation of the accumulated stress after salt leaching has ceased. The predominantly vertical growth evident throughout this structure is interpreted to correlate with subsurface sediments that are subsiding along reverse-fault planes during initial formation. The asymmetry in rock geometries apparent within the overburden on seismic images is a bit unusual for a single borehole-induced dissolution void. Future surface growth will likely correlate with this nonlinear radial-growth pattern observable in the subsidence-altered reflections beneath the sinkhole.

Unique to this sinkhole is the two-well hydrologic system and the nonsymmetrical reflection and bed offset geometries about the principal well bore. It is likely these two unusual situations/characteristics are cause and effect, respectively. This lack of verticality, normally observed in well-induced subsidence features, is also a likely result of this two-well system. The hydrostatic head of the completion units (geologic) for each well would dictate fluid-flow direction (artesian or gravity) and volumes. With the enhanced potential for fluid transport, this two-well system could eventually lead to leached volumes and a subsequent sinkhole significantly larger than any single-well sinkhole currently known to exist.

Careful study of geometries prevalent in this seismic image provides important clues to sinkhole growth and factors influencing areas of active leaching. Bed offsets on the east are markedly different in orientation and general geometry relative to the west side of the structure. Building on the observations on seismic-reflection surveys at subsidence sites previously discussed in this chapter, the more reverse-fault-dominated east side of the structure is likely to support the majority of future subsidence. Implications from previous sites would support the suggestion that normal-fault-controlled subsidence on the west is the response to gradual relaxation of stress over an area without current leaching. On the east, however, the reverse-fault architecture bounding the outermost perimeter of the subsidence volume is one indicator of active leaching and potentially higher subsidence rates resulting in a much larger surface expression.

Working through this collection of borehole-induced dissolution and subsidence features, various development scenarios appear consistent for all structures. First, initial failure occurs along offset planes with reverse (hanging wall above footwall) orientation. Second, based on a single site that was known to have formed catastrophically, a reverse-fault volume defining the chimney structure contains collapse breccia that was generated as a result of rapid material failure. Third, active dissolution and void development with associated collapse will constrain itself predominantly to reverse-fault hed offsets, but during secondary failure these reverse faults will splay off small-scale normal faults near the ground surface. Fourth, during periods of extensional strain, void growth is unlikely and this stage generally appears to represent a decaying energy state. With no confirmed seismic images of subsidence features at the pre-sinkhole development stage and post-initial collapse stage, the migration process toward the surface must be deciphered from available post-sinkhole clues. An investigation of a solution salt-mine roof failure provides images of rock distortion that are likely indicative of roof stoping during compressional-stress-driven failures before sinkhole development.

Catastrophic development of a sinkhole in a dissolution-well field threatening a near-by city street and railroad spur prompted a subsurface investigation which included three 200+-m-long seismic-reflection profiles acquired adjacent to the sinkhole (Table 1 ⑫). The salt interval at this site was about 100 m thick with the top of the salt about 125 m below ground surface.

A clearly definable void-looking feature can be interpreted on the seismic-reflection section beneath station 210 (Figure 18). Seismic characteristics of this void are unique relative to the rest of the reflection events on these data and consistent with expectation (diffractions, scatter energy, out-of-the-plane events, draping-reflection horizons, etc.). The seismic profile was acquired immediately adjacent to the sinkhole but in an area where the ground surface had not yet subsided. Rocks between the salt void and ground surface (overburden) imaged as part of the seismic survey show no evidence of distortion related to the salt void. Considering the seismic-reflection survey only sampled a 2-D slice between the sinkhole and city street, strong seismic evidence exists to suggest this void extends beneath the city street and railroad spur. Drill data designed to ground truth tbese seismic data corroborated the seismic interpretation.

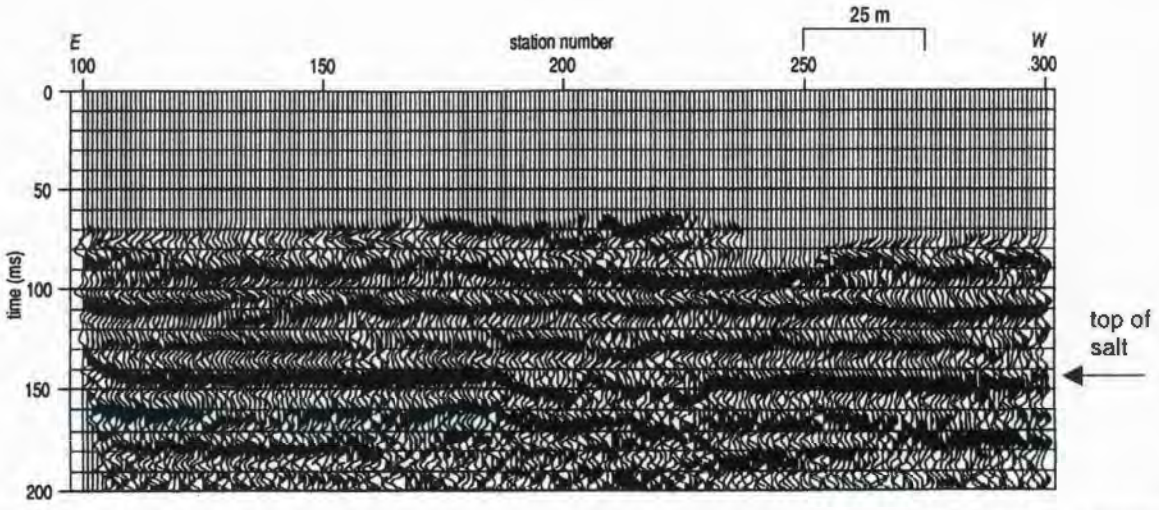

Figure 18. Twelve-fold, CMP seismic section from collapsed dissolution salt well in Hutchinson, Kansas. Disturbed top of salt is evident beneath station 210 at a two-way traveltime of 140 ms, equating to a depth of about 125 m.

Considering the proximity of the seismic line to the sinkhole and the clearly distinguishable seismic signature of the top of the mined salt "jug," it is reasonable to suggest that rock failure between the jug and ground surface was constrained to a very narrow chimney significantly smaller in diameter than the jug. This subsidence geometry is consistent with the concept that initial failure over a void or cavity occurs along the lines of greatest stress defined by the tensional dome. Subtle indications of drape in the imaged overburden appear to narrow as the disturbance moves toward the ground surface—an observation consistent with reverse-fault-controlled subsidence associated with initial failure during leaching and void growth.

Failure of another salt jug in this same mine field (less than 0.5 km away) occurred approximately 10 years after this failure. Seismic and drill data confirmed the sinkhole was the surface manifestation of cylindrical and near-vertical failure in the overburden above a known salt jug. The collapse of consolidated overburden was isolated to a relatively narrow chimney feature (smaller in diameter than the salt jug and narrowing upward) connecting the salt jug with the bedrock surface. This geometry is consistent with the suggestion that initial failure was along or coincident with the lines of equal stress present in rocks above and around a void. Rapid initial growth of the sinkhole after catastrophically appearing was the result of gravity slumping of unconsolidated materials into the 4-m-wide opening at the bedrock surface some 20 m below ground surface.

Summing Up

Working through this collection of natural and borehole-induced dissolution and subsidence features presented in this document, various development scenarios appear consistent for all structures. First, initial failure occurs along reverse-style offset planes (hanging wall above footwall). Second, multiple groupings of reverse-fault planes relate to episodic collapse due to active dissolution. Third, the innermost reverse-fault pair maps the tensional dome and initial chimney feature possessing catastrophic-collapse potential. Fourth, during secondary failure associated with active leaching, reverse faults will splay off small-scale normal faults near the ground surface. Fifth, normal-fault geometries designate a low-energy stage in terms of active dissolution and collapse rates. Sixth, during periods of extensional strain, void growth is unlikely and this stage generally appears to represent a decaying energy state. Juvenile subsidence structures inferred from seismic images have characteristics that support the upward migration of a dissolution void as interpreted from drill investigations at dissolution mines and deciphered from seismic images of post-failure structures.

References

Lambrecht, J.L., and R.D. Miller, 2006, Catastrophic sinkhole formation in Kansas: A case study: Leading Edge, v. 25, n. 3, p. 342-347.

Miller, R.D., 2003, High-resolution seismic-reflection investigation of a subsidence feature on U.S. Highway 50 near Hutchinson, Kansas; in, K.S. Johnson and J.T. Neal, eds., Evaporite Karst and Engineering/Environmental Problems in the United States: Oklahoma Geological Survey Circular 109, p. 157-167.

Miller, R.D., 2006, High-resolution seismic reflection to identify areas with subsidence potential beneath U.S. 50 Highway in eastern Reno County, Kansas: Symposium on the Application of Geophysics to Engineering and Environmental Problems [Ext. Abs.]: Selected as a best paper from SAGEEP06, presented at Near Surface 2006, Helsinki, Finland, Sept. 4-6, 5 p. (published on CD).

Miller, R.D., D.W. Steeples, and J.L. Lambrecht, 2006, High-resolution seismic-reflection imaging 25 years of change in I-70 sinkhole, Russell, County, Kansas [Exp. Abs.]: Society of Exploration Geophysicists, Tulsa.

Miller, R.D., D.W. Steeples, and J.A. Treadway, 1985, Seismic reflection survey of a sinkhole in Ellsworth County, Kansas [Exp. Abs.]: Society of Exploration Geophysicists, Tulsa, p. 154-156.

Miller, R.D., D.W. Steeples, L. Schulte, and J. Davenport, 1993, Shallow seismic reflection study of a salt dissolution well field near Hutchinson, Kansas: Mining Engineering, October, p. 1291-1296.

Miller, R.D., A.C. Villella, and J. Xia, 1997, Shallow high-resolution seismic reflection to delineate upper 400 m around a collapse feature in central Kansas: Environmental Geosciences, v. 4, n. 3, p. 119-126.

Spinazola, J.M., J.B. Gillespie, and R.J. Hart, 1985, Ground-water flow and solute transport in the Equus beds area, south-central Kansas, 1940-1979: U.S. Geological Survey Water-Resources Investigations Report 85-4336, 68 p.

Walters, R.F., 1980, Solution and collapse features in the salt near Hutchinson, Kansas: Geological Society of America, South-central Section, Field Trip Notes, 10 p.